Marshall Plan Scholarship Program
Report

Applicant   DI Stefan Strohmeier (PhD Student)
University of Natural Resources and Life Sciences (BOKU) Vienna, Institute of Hydraulics and Rural Water Management, Department of Water, Atmosphere and Environment, Muthgasse 18, 1190 Vienna, Austria

Hosting Dept.   Department of Agronomy, Lilly Hall of Life Sciences, 915 W. State Street, Purdue University, West Lafayette, IN 47907-2054

Research Proposal (MPS Program Application)

Analyzes and Simulation of rainfall driven Soil Erosion

Final Project Title

Experimental Rill Erosion Development Study

Acknowledgement

Index

1.) General Project Overview

This report is produced as an agreement between the MPS and the research study performing student (DI Stefan Strohmeier) as program applicant to confirm the scientific content of the abroad research project. The results of the relating study should be used as source for additional research operations and publications to benefit from the experiences and techniques expansively.

According to the branch of study of environmental engineering and soil sciences – primarily soil erosion processes – the proposed focus was set on experimental soil erosion studies. A central institution dealing with the above mentioned tasks on international level is the National Soil Erosion Research Laboratory (NSERL) in collaboration with the Department of Agronomy at the Purdue University. In this way, the decision was to project a research study at the Department of Agronomy using available laboratory sources provides by the NSERL.
According to these opportunities the proposed research project for MPS application in April 2011 was titled "Analyzes and Simulation of rainfall driven Soil Erosion".

Based on the on site conditions at the Department of Agronomy respectively the NSERL the research proposal was discussed and adapted appropriately. The original aim to focus on both – experimental laboratory studies and the acquisition of a computer based erosion modelling tool (GeoWEPP software) was changed in a way to focus primarily on experimental and physical soil erosion trials. The final determination was to adopt physical (experimental) erosion studies to I.) get a better understanding in physical erosion processes, to II.) extract empirical parameters comprised in process describing hypotheses and to III.) analyse empirical/physical formulations also used in GeoWEPP software concerning to the need for adaption due to experimental results.
Because of the usability of high performance research equipment at the NSERL this containment seems to be eligible. The GeoWEPP software is performable by means self organized computer training and detailed user manuals available. Integrated treatment of experimental data and the application in simulation software (GeoWEPP) is achieved through analyzing formulas and assumptions used in the software, calibrated by means of laboratory experiments.

Listed Overview

MPS Applicant: DI Stefan Strohmeier, PhD Student at the Institute of Hydraulics and Rural Water Management, Department of Water, Atmosphere and Environment, BOKU, Vienna

MPS Project Title: "Experimental Rill Erosion Development Study"
Research Proposal Title: "Analyzes and Simulation of rainfall driven Soil Erosion"

Location: Department of Agronomy at the Purdue University and the USDA ARS NSERL situated at the campus of the Purdue University, West Lafayette, Indiana, USA

Project Duration: The study started on Monday 1st of August 2011 and ended on Monday 31st of October 2011 (3 month project duration)

Project Coordinators: Dr. Andreas Klik from the BOKU University Vienna, as supervising Professor of the MPS applicant DI Stefan Strohmeier and Dr. Chi-Hua Huang Docent Professor at the Department of Agronomy and director of the NSERL at the Purdue University as hosting Professor.

2.) Abstract

Using common catchment size erosion model software either lack of knowledge or lack in process ability of watershed characteristics leads to increasing simplifications in model assumptions. Referring to open channel hydraulics, erosion model equations are prevalently based on stepwise uniform flow condition requirements. Approaching balance of gravitational and frictional resistance forces, channel roughness is fundamental model input. The fusion of simplified model assumptions and the use of lumped roughness determination cause ambivalence in model calibration.

By means of a physical model experiment at the National Soil Erosion Laboratory (NSERL), West Lafayette, USA, channel roughness was itemized into skin friction and channel shape friction due to rill morphology. Particularly the Manning-Strickler equation was analyzed concerning the applicability of constant and holistic factors describing boundary friction impacts. The insufficiency in using the Manning-Strickler equation for non-uniform flow conditions is widely advised, whereas lack in predictability in rill erosion development inhibits proper model adoptions. The aim of the present study is to determine the impact of channel morphology on roughness assessment in rill erosion scale.

Therefore a 1.9 meter long, 0.6 meter wide and 0.3 meter deep flume with an inclination of 10 % was filled with a loamy soil representing a section of a hill slope. The soil was prepared and saturated by simulated rainfall before each model run. A single erosion channel was enforced to develop by means of steady state runoff. Two different erosion channel types were initiated and observed: I.) a Straight Constrained Rill (SCR) shape by concentration of the runoff into a prepared straight initial rill and II.) a Free Developing Rill (FDR) by back-cut erosion through the plain soil body. Discharge of the outflow was measured in 5 minute interval and outflow sediment concentration was measured every minute. A top view stereo camera setup was installed to detect the channel topography whereas additional channel width and knick point depth measurements were undertaken manually. Flow velocity was measured at different channel development stages using colour tracer.

Based on the measurements the comparison of flow conditions of different channel types was enabled. Assuming the flow conditions are described by the Manning-Strickler equation adequately, the extracted roughness factor for the SCR is influenced by skin friction only, whereas the FDR holistic roughness factor consists of both - skin and shape friction.

By means of the rill erosion study a significant dependency of Manning-Strickler roughness factors and the developed rill morphology was observed. The experimentally extracted roughness values related to skin friction only (SCR) are up to 30 % higher than the roughness values out of the FDR experiment.

Disregarding criticism about common channel flow equations used in erosion models, experimental studies may provide fractional explain-ability of holistic constants and diminish uncertainty in parameter estimations. The present study shows rill roughness characteristics under specific conditions – varying the experimental conditions reasonable predictions for estimating the rill morphological impact may result.

3.) Introduction

3.1.) General Issues in Soil Erosion

<u>Definition of "Soil"</u>
Soils are complex mixtures of minerals, water, air, and organic matter (both dead and alive), forming at the surface of land. The soil performs many critical functions in almost any terrestrial ecosystem (whether a farm, forest, prairie, or suburban watershed) (ASA-CSSA-SSSA, 2011). Soil as upper layer of the lithosphere provides a wide range of an-organic and organic sources with major effect on terrestrial life an environment.

<u>Definition of "Soil Erosion"</u>
Soil erosional loss is caused by wind, water, ice and movement in response to gravity. Although the processes may be simultaneous, erosion is distinguished from weathering. Erosion is an intrinsic natural process, but in many places it is increased by human land use. Poor land use practices including deforestation, overgrazing and improper construction activity. Improved management can limit erosion by using techniques like limiting disturbance during construction, avoiding construction during erosion prone periods, intercepting runoff, terrace-building, use of erosion-suppressing cover materials, and planting trees or other soil binding plants (Wikipedia, 2011).

Generally, soil erosion consists of the processes of destabilization, detachment and transport of base material. All Processes can be caused by similar impact – but not in every case. Aside from water, wind and temperature impacts on soil erosion, vegetation, microorganisms, tillage, harvesting, e.g. can play a mayor role too.
A soil erosion problem appears if the soil in situ conditions (soil surface, slope, vegetation, …) allow the driving forces (rainfall, motion of water, …) to erode soils with specific demand (agricultural, settlements, …) only.

<u>Soil Erosion by Water</u>
Appearance:

Identification	**Development**
Sheet Erosion / Interrill Erosion	Raindrop Splash Erosion, Sheet Flow Transport
Rill Erosion	Local Concentration of Runoff, Channel Formation
Gully Erosion	Advanced Stage of Channel Erosion
Permanent Channels, Rivers	
Debris Flows	
…	

Problems:

On – Site	**Off – Site**
Soil Loss	Accumulation of fine Material
Loss of Nutrients	Covering of Infrastructures
Reduction of Water Storage Layer	Damage of Constructions
Excavation of Roots	Siltation of Reservoirs and Lakes
Damage of Vegetation	Eutrophication of Surface Water
Corrugation of Fields	Accumulation of Pollutants
Interruption in Cultivation	…
…	

Fig. 1. Degraded land in Ethiopian highlands

Fig. 2. Siltation of a hydropower reservoir (China)

Processes:

Process	Erosion-Effect	Additional Effects
Raindrop Impact	Breakup and Detachment of Surface Soil Aggregates	Clogging of Soil Pores
Sheet Flow Interrill Erosion	Transport of detached Soil Particles, Splash	Sealing of Pores, Attachment of "coarse" Particles (Layering)
Channeling Rill Eroison (cons. Gully)	Transport of Interrill yield, Channel Erosion	Aggregation of Interrill System, back-cutting

Model Explainations:

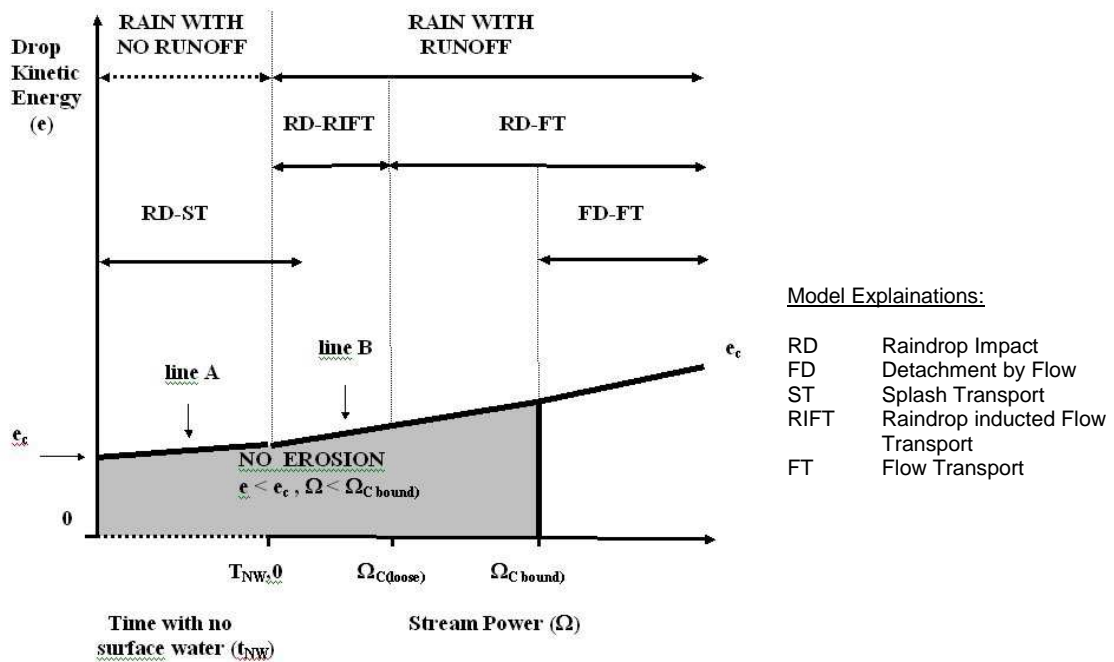|	
RD	Raindrop Impact
FD	Detachment by Flow
ST	Splash Transport
RIFT	Raindrop inducted Flow Transport
FT	Flow Transport

Fig. 3. Interactions (schematic) between raindrop impact and flow impact by P.I.A. Kinnell (2005)

4

3.2.) Project specific Issues in Soil Erosion

The focus of the present study is on channel erosion processes. The aim of the "Experimental Rill Erosion Development Study" is to analyse I.) the concentration of the shallow sheet surface flow into defined channels, II.) the development of erosion rills as a back-cutting process and III.) the channel flow conditions in direct comparison of straight constrained rill (SCR) to free developing rills (FDR).

For catchment soil erosion modelling purposes, rill and emepherial gully processes – if considered at all – are calculated by means of simple and well established river hydraulic modelling approaches mainly. This causes problems as "accurate" modelling routines provide more or less "accurate" data input concerning the boundary and initial conditions. Detailed knowledge about rill network development and consequential surface flow conditions are rarely available in most cases. Thus, global assumptions have to be defined with certain effect on model output. The variance of global assumptions - particularly roughness assumptions as driving forces concerning soil resistance, and back-influencing the channel flow conditions - are main focus of this study.

Channel Erosion Processes

Channel erosion is caused by the attacking forces of concentrated water flow acting at the channel boundaries. Also the sediment transport caused by interrill erosion (from shallow sheet flow) joining the channels has to be taken into account. The turbulence in the channel flow is enabled to transport a certain sediment concentration – exceeding this contingent, additional sediment will settle down and cause deposition. This phenomenon is described by the law of sediment transport capacity.

During the channel development, the upper point of flow concentration produces headcut erosion. A headcut is a step change in bed surface topography where intense, localized erosion takes place (Bennet et al., 2000). It has been observed, that rill incision and high rates of soil erosion are the result of headcut development and migration in laboratory channels (Robert R. Wells, 2009; Slattery and Bryan, 1992; Brunton and Bryan, 2000).

Channel Flow Hydraulics:

For describing the flow characteristics in open channel flow, different empirical and physical relations for different scale depending on the accuracy of available data were investigated. In general, physical relations are based on mass balance laws and the relation of acting forces respectively energies.
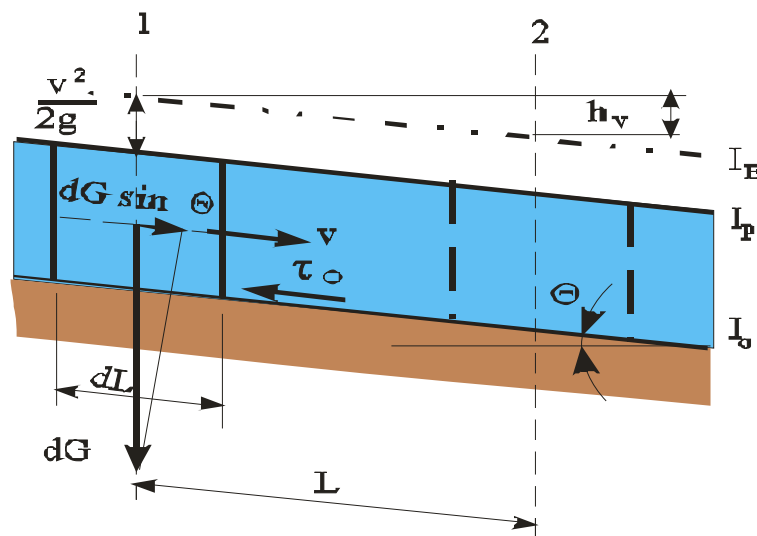

Fig. 4.   **Longitudinal Channel Flow Intersection: Acting Forces and Parameters (Loiskandl, 2011)**

Law of equality of forces (mass force=friction force)

$$F_G \sin\theta = F_R \qquad [1]$$

From this basic principle, following equation can be derived:

$$v = \sqrt{\frac{8g}{\lambda}} \; \sqrt{\frac{A}{U}\frac{h_v}{l}} \qquad [2]$$

Flow formula of *Brahms-De Chezy*:

$$v = C \; \sqrt{R\,I} \qquad [3]$$

And the simplified flow equation after *Gauckler-Manning-Strickler*:

$$v = k_{st} \cdot R^{2/3} \cdot I^{1/2} \qquad [4]$$

Formula [4], the *Gauckler-Manning-Strickler* equation is a simplified relation for estimating the channel flow based on the parameters v (mean channel flow velocity), R (hydraulic radius), I (slope of the channel) and k_{st} (*Strickler-Roughness-Coefficient*) which is used as holistic factor to estimate the friction component.

Scientists indicate the character of the formula as a tool of flow estimation as there is insufficiency in using equation [4] with constant k_{st} for different hydraulic conditions. Equation [4] was developed for steady state and more or less uniform channel geometry conditions.

Another aspect is the lack of knowledge in the development of the rill erosion system. Accurate rill channel geometries in large scale catchments are not predictable by means of up to date erosion modelling software. Moreover, ephemeral gullies can grow rapidly in size within individual storm events, thus representing areas of intense, localized scour that may not be predictable using current modeling paradigms (Valentin et al., 2005).

Because of its simplicity in use and the task for a single parameter (k_{st}) only, equation [4] is widely and commonly used in channel hydraulic aspects concerning erosion modelling up to date. From the point of view of dealing with unconfident predictability concerning channel morphology the practicability of using advanced physically based flow formulations might be questioned anyway.

Channel Erosion:
Traditionally, most channel erosion equations are based on hypotheses of exceeding critical forces of channel boundary resistance. Once the acting force (channel water flow) exceeds the soil resistance force, erosion occurs. The critical point of starting motion of sediment is subject of interpretation, as soil consists of different particles size, density, shape, cohesion potential e.g. In this way the formulation of a certain value might be questioned. Anyway, the hypothesis of critical value is commonly used in a wide field of application.
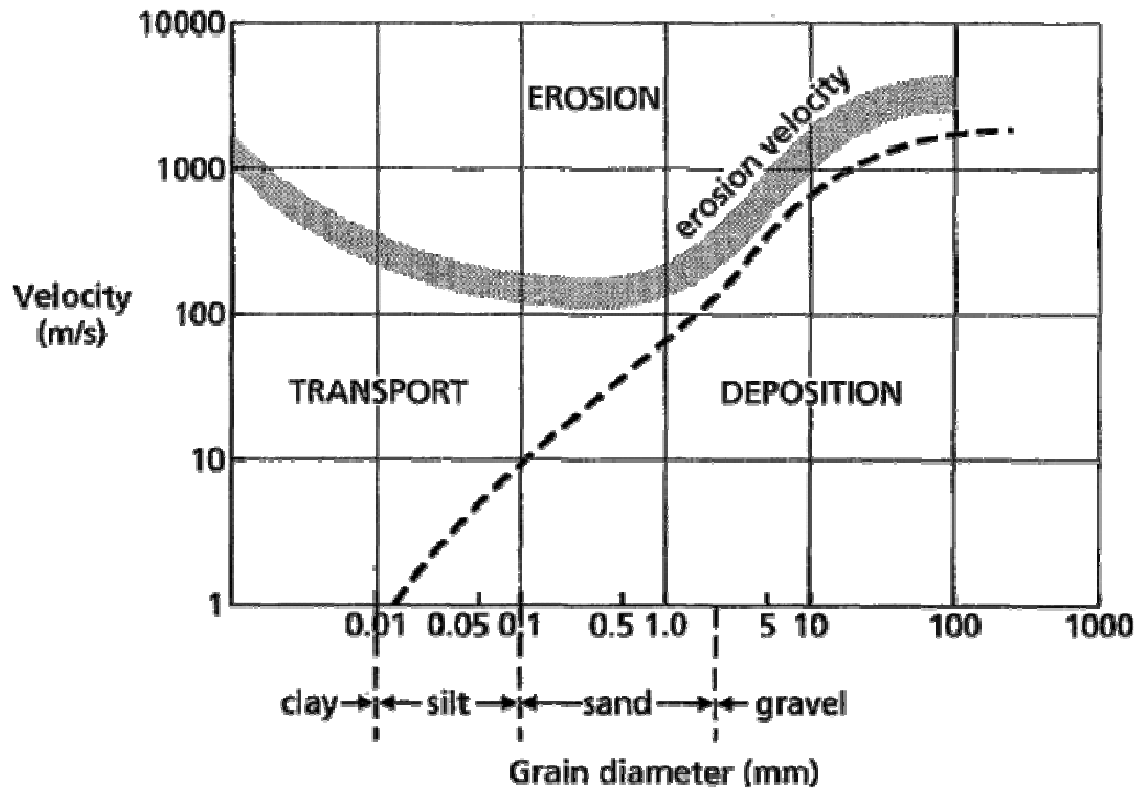
Graph 1. Critical value for beginning of motion: Hjülström Diagram (critical value = v)
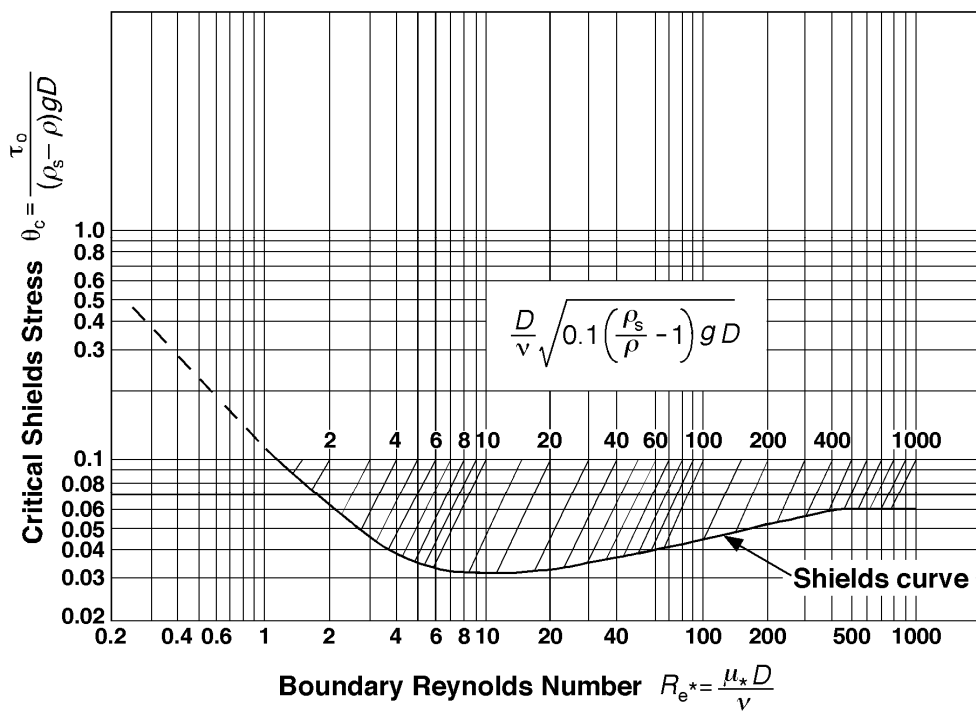

Graph 2. Critical value for beginning of motion: Shields Diagram (critical value = Shields parameter)

7

Graph 1 and 2 illustrate relations of critical values. A often used definition of critical value is the critical boundary shear stress (indirectly incorporated in the *Shields Parameter*).

Assuming hydrostatic conditions in the water body, the shear stress *T* can be derived as follows:

$$\tau = \rho \cdot g \cdot R \cdot I \qquad \text{[5]}$$

$\tau_f < \tau_c \rightarrow$ no erosion
$\tau_f < \tau_c \rightarrow$ erosion
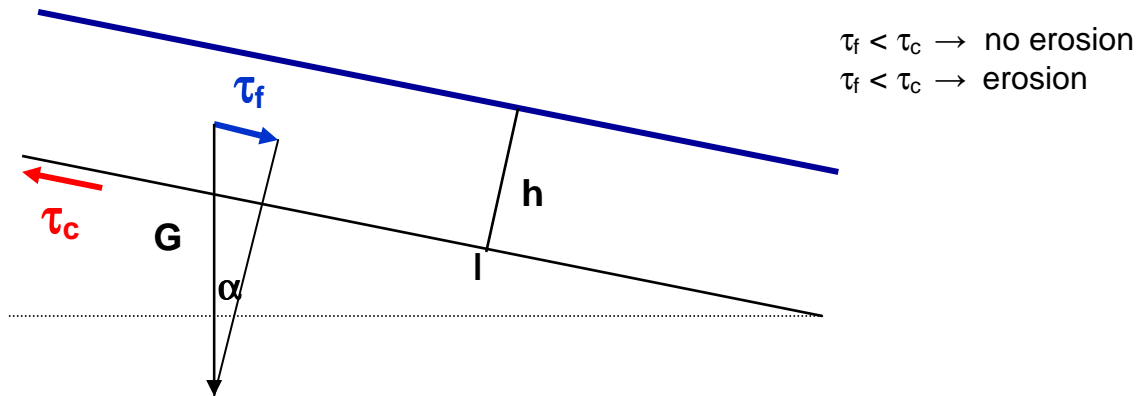
The widely approved erosion modelling software WEPP (Water Erosion Prediction Project) developed at the NSERL, West Lafayette also uses *T_{crit}* and *Gauckler-Manning-Strickler* assumptions for calculating channel erosion.

Following definition for channel erosion computation is given in the WEPP user manual (Flanagan et al., 1995):

$$D_c = K_r \cdot \left(\tau_f - \tau_c\right) \qquad \text{[6]}$$

D_c Detachment Capacity by Rill Flow (kg.s^{-1}.m^{-2})
K_r Rill Erodibility (s.m^{-1})
τ_f Flow Shear Stress (Pa)
τ_c Critical Shear Stress (Pa)

As mentioned in sub-chapter of Channel Erosion, the scouring power of the water is assumed to be limited by the sediment transport capacity. There are different hypothesis of assuming the sediment transport capacity. Following equation is illustrated in WEPP user manual (Flanagan et al., 1995):

$$T_c = k_1 \cdot q^\beta \cdot S^\gamma \qquad \text{[7]}$$

T_c Transport Capacity by Rill Flow (kg.s^{-1}.m^{-2})
k_1 empirical constant
q Discharge per unit width (kg.s^{-1}) or (m^3.s^{-1})
S Slope gradient (m.m^{-1})
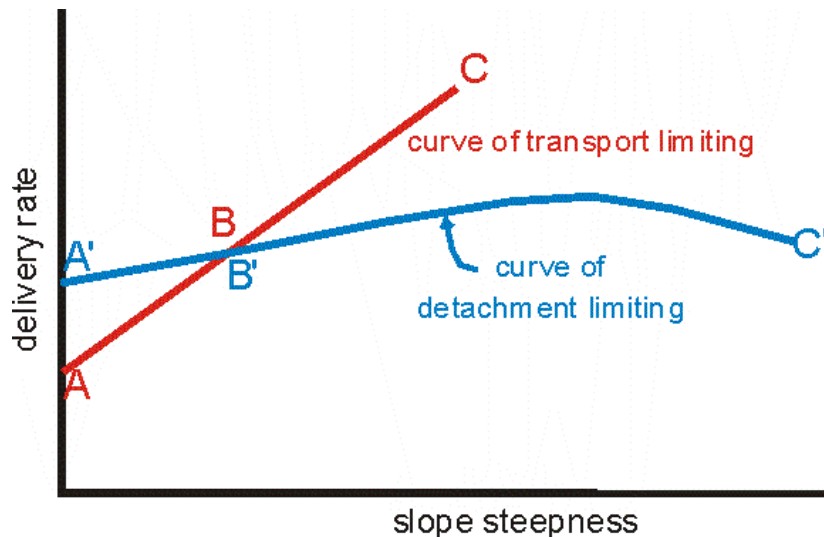
Graph 3. Law of sediment transport capacity – delivery rate to slope steepness

Project Specific Focus

In chapter 3.2 and subchapter "Channel Erosion Processes" general channel erosion aspects were discussed. With the aim to point out the significance of small scaled rill morphology, physical based relations were analysed further. The approach was to observe the hydraulic conditions of the flow and erosion behaviour in the model flume. Knowing the boundary conditions, the observations are back-calculate able by means of established hypothesis mentioned above. Comparing rills with and without shape roughness influence – the back-calculated holistic roughness values are assumed to be explainable by the rill morphology. The actual stage of analyzes and the corresponding hypotheses are shown in chapter 5.1 Introduction in Results and Analyses (Current Stage).

4.) Materials and Methods

4.1.) Experimental Setup

General Terms in physical Modelling

Adequate definition of experimental setup is essential issue. The aim for setting up laboratory tests is to reproduce simplified natural phenomena knowing boundary and initial conditions. It is assumed, that simplified models are able to represent and detect most significant processes. As physical models represent the nature fractionally only, the results out of the trials have to be up-scalable. This might be criticial issue, as the geometric scale of a model is not coactively linear with up scaling of forces. From physical view on natural processes like flow and erosion, hypotheses are often based on "equality of forces assumptions" e.g.

As a complete similarity between two systems is not reproduce able, the aim is to look for partial similarity. As a consequence, the parallel reproduction of physical, chemical and biological occurrences in one global model cannot be constituted due to physical modelling (Loiskandl, 2011).

The scale ability of models is limited onto fractional issues, wherewith insufficiencies concerning relations of forces appear. Particularly, the physical relations after *Froude* and *Reynolds* concerning channel hydraulics are not (resp. hardly) compatible. Both relations are describing open channel flow conditions but both behave divisively due to changes in model scale.

Fortunately, in aspect of rill erosion modelling natural phenomena are applicable by means of model experiments in realistic scale. Occurring erosion rills during model tests might occur under field conditions in comparable morphology. However, limitations flume geometrics are of influence as natural hill slopes are significantly longer – and boundary conditions of course may differ.

Rill Development Study Set Up at the NSERL
The entire aim of reproducing rill erosion was projected by means of flume experiment analyzes. Various prior test runs (Aug 2011 until mid of Sept 2011) were performed to define final model setup. The adjustment of boundary and initial conditions during prior runs and changes in setup are critical point. To determine the significance of single parameters a wide range of the parameter values has to be analyzed. By means of variation in run conditions, reliable regressions and determinations in behavior might be conclude able. On the other hand, through limitation in scale and impact of boundary conditions variation of parameters is limited too. For example: Increase in flow discharge causes rise in water table of the channel flow whereas the stream will reach the metal sheet boundary of the flume at certain stage. In this case the boundary roughness of soil is no longer assumable as the channel flow is toughing the plain surface of steel.
In this manner the prior setup adjustment is indispensable, sensitive and time consuming point.
The final experiment run setup has been scheduled in mid of Sept. 2011. Regarding to the technical advice of Dr. Huang - Dr. Klik, Dr. Norton we defined run setup and series as described in following chapter.

a.) Flume Setup
b.) Soil Setup
c.) Experimental Run Setup

a.) Flume Setup
The flume construction for the present "Experimental Rill Erosion Development Study" at the NSERL was based on an existing flume pan of 4.50 meter length, 0.25 meter depth and 0.60 m width. Figures 5 to 8 provide additional information concerning the following description of the flume construction.

Based on prior tests and the availability of test soil, it was decided to limit the flume length by 1.90 meter. As the flume drainage system was agreed to project under free drainage conditions, bottom holes in the flume pan and a ground gravel layer were designed. Because of the need for an erodible soil layer and the control of the water infiltration conditions, the steel sidewall boundaries were extended to 0.30 m height. At the flume outlet a front plate with central outlet opening (5 cm width at the bottom, and 60° widening trapezoid) was fixed. In this way, the outflow of the flume was controlled in shape and channel bottom height. The soil surface was prepared up to a height of 5 cm above the fixed outlet opening. Based on this scouring and back-cutting erosion is induced. Downstream of the outlet panel, a steel water funnel was fixed to define the water outflow and provide sediment sample collection below the flume outflow.

The flume-inflow was designed as a well construction. The metal well construction acts as water reservoir and was planed to equalize inflow and prevent against short term water pipe fluctuations. The inflow tube connected to tab water system was fixed at the reservoir. At the outlet of the upstream water reservoir, a flat and wide trapezoid opening was cut in the metal boundary to provide uniform surface inflow onto the plain soil body in the flume. In addition, a protecting fleece textile was fixed at the reservoir outflow to prevent against pothole erosion at the upper soil flume

boundary (Fig. 5 to 8). The whole construction was attached on a brick base frame at the concrete floor of the laboratory to adjust the flume in a certain angle (soil surface slope).

A natural soil layer was reproduced by means of a 10 cm thick gravel layer at the flume bottom and a 15 to 20 cm thick top soil layer above. Between the two layers a protecting filter textile was added.

Geometry

Length	1.9 m			
Width	0.6 m			
Depth	0.3 m	- Ground drainage	0.10 m	(Gravel+Bricks)
		- Soil layer	0.15-0.20 m	(Soil)

Inclination
Flume Slope   5.7°(10%)

Fig. 5.   Flume Setup: View into the plain steel flume

**Fig. 6.   Flume Setup Preparation:
  "Ground Drainage" layer
  (Gravel & Bricks)**

11

Fig. 7.   **Flume Setup Preparation: Soil layer with textile protection**

Fig. 8.   **Final Setup**

b.) Soil Setup

<u>Soil Type</u>
Topsoil: Laom soil from "Bennet Company", grinded < 2cm. Fractional stones and organic matter implemented.

<u>*Soil Texture:*</u>
Sand   32%
Silt   49%   *Loam*
Clay   19%

The soil texture analysis was done at the NSERL by Hydrometer Method and 3 replications. The Hydrometer Method is based on the settling velocity of solid particles in a fluid considering *Navier Stokes* law. The standard method of the hydrometric measurement is applied in a modified procedure at the NSERL, West Lafayette. By measuring fluid density in the sample bottles 2 times (after 40 seconds and 24 hours) at defined bottle depth, the proportion of solid particles at the measurement point is recalculate able. Trough assignment of related particle diameter, the soil texture can be detected.

<u>Soil Assembly</u>
A 15-20 cm thick topsoil soil layer was prepared by dumping soil buckets onto the protection foil above the ground gravel layer in the flume. Slight soil compaction through low pressure hand respectively small scoop and shape panel treatment was performed.

1. Free Development Rill (FDR)　　Shape Panel Treatment:
35 cm of Plain Horizontal Surface (Erosion Area)
12.5 cm of Steep Side Board Soil, incl.= 40%
(left and right)

2. Straight Constrained Rill (SCR)　　Shape Panel Treatment:
35 cm of Plain Horizontal Surface
12.5 cm of Steep Side Board Soil, incl.= 40%
(left and right)
+ Trapezoid Central Channel:
a=4cm, c=12cm, height=4cm

Fig. 9.　FDR Soil Setup: rreparation of the soil surface by metal shape panel

Fig. 10.　View into the flume: the soil surface preparation is plain and rough by grain diameters

Fig. 11.　Free Development Rill (FDR): soil preparation is uniform plain

Fig. 12.　Straight Constraint Rill (SCR): initial channel in the centre of the thalweg

Soil Pre Conditions

The soil got assembled under air dry conditions. After shaping the soil surface with the shape panels, rough tracks of panels were erased and a thin layer of additional soil was sprinkled on top. Thus, a soil specific (<2 cm grinded) rough surface at the leveled and leveled bed was prepared.

Afterwards, two hour rainfall treatment for smoothen up the surface and to allow soil compaction by gravitation as well as to seal the surface through flushing small particles into the pores was executed. The constant pre-wetting rainfall intensity was about 1.25 cm per hour.

After two hours of rainfall, one hour of resting time for compaction processes and drainage water into deeper soil zones was awaited.

The run was projected to be executed under free drainage conditions - therefore the gravel bed was designed as ground layer.

Fig. 13. Soil Pre Conditions:
soil surface after 1 hour of rainfall and
2 hours of resting time

Fig. 14. Soil Pre Conditions:
detail of the soil surface, smoothened and
washed out relief – fine material clogs surface

Bulk Density

Bulk density is important soil condition describing parameter. Therefore core samples of the soil were taken out of the flume. The compacted soil after rainfall treatment and the experimental run was taken in three different runs. The core cylinder was of 12.4 cm in diameter and 7.5 cm height. The soil samples were oven dried by 105°C (standardized) and weighted afterwards. Relating dry soil mass to the volume of the core sample, the bulk density can be computed as follows:

$$\rho_d = \frac{m_d}{V_{Cyl}}$$

[8]

P_d Bulk Density (g/cm³)
m_d Dry Mass of the Soil (g)
V_{Cyl} Volume of the Core Sample Cylinder (cm³)

Bulk Density: 1st test 1.39 g/cm³
                 2nd test 1.42 g/cm³   *Mean Bulk Density: 1.41 g/cm³*
                 3rd test 1.42 g/cm³

c.) Experimental Run Setup
Concerning flume laboratory experiments several parameters of impact can be adjusted:
- Flume size
- Inclination
- Discharge
- Soil (type, preparation, grinding size, density, tillage, pre-events, time....)
- Soil boundary conditions (free drainage, seepage...)
- Surface preparation

Because of limits in time and soil amount the decision was to concentrate on one flume size, soil and soil boundary condition. Because of the need for run replications, the slope was held constant too, to reduce the required number of runs.
Following experimental set up was chosen (parameters):

Constant: Flume, inclination, soil, soil boundary condition
Variable: Discharge, surface preparation

Final Run Setup:
Surface preparations	2	FDR, SCR
Discharges	2	0.145 and 0.270 l/s
Replications	3	
Total	12	Runs

4.2.) Data Reprocessing Methods

Overview of Measured Data
The test flume was set up directly below laboratory rainfall simulator elements to produce soil saturation conditions as well as to create a smooth soil surface. After the rainfall treatment, a stereo camera setup consisting of two computer controlled cameras was positioned in top view to the flume centre. In this way continuous observation – in one minute photo intervals – of the rill morphological development was enabled. By means of the stereo-camera setup, 3D photogrammetric analyzes are enabled to reproduce channel geometries. Channel shape information is essential input for flow hydraulic calculations. Furthermore, discharge, velocity and sediment concentration measurements were undertaken.

Measured Data:
Setup Conditions
- Flume Geometry (Length, width, depth, surface, slope)
- Soil (Type, texture, preparation, drainage system = free drainage)
- Initial Conditions (Discharge, soil saturation and surface treatment, soil bulk density)

Run Measurements
- Channel Geometry (Development):
  - Stereophotos; 1 min. interval
  - Manual channel geometry measurement; 5 min interval
- Discharge:
  - Inflow (adjusted)
  - Outflow; 5 min. interval
- Flow Velocity:
  - Shallow surface flow velocity by color tracer measurement before channel incision (FDR); 5 min. interval

- Channel flow velocity by color tracer
(SCR, FDR – after channel incision); 5 min. interval
▪ Sediment Concentration
- Sediment conc. by means of 1 liter bottle samples; 1 min. interval

The schedule above illustrates setup conditions of the experiment as well as measured data during experimental runs. The Setup Conditions are discussed in chapter "Rill Development Study Set Up at the NSERL" in detail. The "Run Measurements" are explained in the following episodes:

Channel Geometry
The channel geometry development is essential due to rill erosion and sediment transport. The back-cutting erosion loosens up the soil material - the so called knick-point of the channels. The eroded material is transported downstream by the channel flow up to certain transport capacity (relation: [7]). Also flow hydraulic conditions in the rills are significantly co-determined by channel geometries. Particularly in case of testing the *Manning-Strickler* hypothesis, knowledge about flow geometry is essential.

The channel geometry measurement was executed manually by hand measurement as well as by means of photogrammetric analyses. The manual measurement focussed on channel length, width and knick point depth in 5 minute interval measurement. During the FDR experiment, the knick-point back cut erosion and rill development started with the beginning of the experiment. During SDR test runs sudden scouring in the channel bed of the initial rill occurred. In this case, the manual measurement method was executed to monitor stereo-photo analyses only. However, the analysis of the present report is based on manual geometry measurements by hand, as the photogrammetric processing is not finished yet.

The stereo-photo monitoring was provided by a stereo-camera application under flume top view conditions. Two computer controlled cameras were positioned on a float arm approximately 2 meters above the flume construction. The overlap area of the images of both cameras was about 1.25 meters in length out of the 1.90 m long flume model.
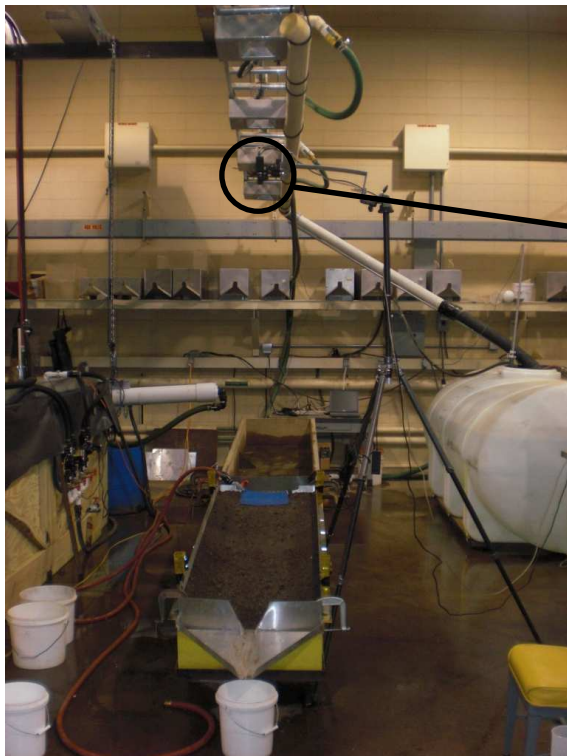
Stereo-Photo-Camera
Two computer controlled cameras were situated in the centre of the flume. In this way a 1,25 m long section of the rill-channel was observed by means of two camera images. The image data was saved in one minute interval. Based on photogrammetric analyses, digital DEM`s are produce able. These DEM`s describe channel geometries of rill erosion occurrences.

Fig. 15.   Stereo-Camera Setup

The major advantages of automatic and remote sensing geometry observations are in the consistent and spatial smoothed monitoring possibility disregarding influences due to detection and model interference. Gauge measurements e.g. provide single point data only. Changing river boundary conditions due to downstream moving dune occurrences, the surface flow structures (waves) will move as well. Concerning such kind of local phenomena, local measurements may vary time depending. Local phenomena can be smoothened out by means of larger scale monitoring lengths (areas). Specific concerns like channel meandering (rill tortuosity) might be analysed using GIS tools. Photogrammetric monitoring provides large data amount usable for further analyses.

Discharge
The inflowing discharge is controlled by a plug valve at the tab water tube connection. The adjustment of the plug valve was calibrated before every experimental run. The discharge adjusted tab water flows into the upstream water reservoir. After fulfilling the water reservoir the outflow through the flat trapezoid opening is entering the fleece textile protected soil surface. The fleece protects against scouring erosion at the reservoir overflow and provides uniform distribution of surface water at the flume inlet. The adjusted inflow discharges were 0.145 liter per second and 0.270 liter per second.
The flume outflow was controlled by 10 second bucket measurements to measuring intervals of 1, 2 and 5 - and every 5 more minutes. Knowing the inflow and controlling the inflowing water after the experiment for consistency, the water balance can be derived. The exceeding water of the inflow of the measured outflow is caused by water storage in the soil layer as well as leakage water. Based on the water balance graph, stable state water leakage concerning soil and boundary conditions may be assumed.

Flow Velocity
As flow velocity is connective parameter between discharge and the cross sectional channel geometry, accurate measurement of the mean flow velocity is essential. The measurement of the mean flow velocity is executable different way. Common methods are local point measures by means of flow propellers, ultrasonic or radar based e.g. or channel flow smoothened by use of tracer liquids. For present experiment tracer method was applied. The big advantages of the tracer method are none (or low) influence on channel processes during measurement and the smoothening of local flow phenomena due to a certain flow length. The flow path length related to the travel time of the tracer covers a certain section of channel flow and local phenomena like changes in hydraulic regimes from under critical to supercritical get flattened out.
Concretely, a green food colour tracer was used between upper and lower control cross lines (Fig. 16, 17). The travel time of the colour was measured by chronograph and related to the travel path – not the direct distance between the cross lines, but the analyzed flow morphology based on the top view photos of the stereo-camera setup. To take into account the dispersion of the colour front of the tracer, several studies have been undertaken about this phenomenon. Different scientific advices are available how to handle the colour dispersion – in general they agree with not using the colour front for defining the mean flow velocity. During the channel experiment measures the top of a strong coloured fraction of colour flow was used to estimate the average flow velocity – which was about ca. 0.8 times the colour flow front.
In the present study two different types of surface flow were monitored. The first flow type describes the uniform and shallow surface flow over the plain soil surface which occurs in under FDR conditions in the beginning stage only. Later, after scouring at the bottom outlets knick-point (as the soil surface is about 5 cm higher than the downstream channel outlet) back-cutting erosion occurs and this channel development starts. When the shallow surface flow concentrates in the back-eroding rill, channel flow is developing downstream. Thus, the FDR type provides 2 types of flow conditions and also 2 different stages of flow velocity measures (Fig. 16, 17). The hydraulic flow situation changes during channel formation. In this way the measurements of the flow velocity were executed in 5 minute interval, to

observe time related behaviour of flow conditions. In this way, temporal geometry, flow conditions and roughness has to be taken into account.

The SCR type provides channel flow hydraulic situation only. Although the channel formation happens under SCR conditions too, the flow is always channel flow. During the SCR experiment, the flow velocity was measured every 5 minutes.
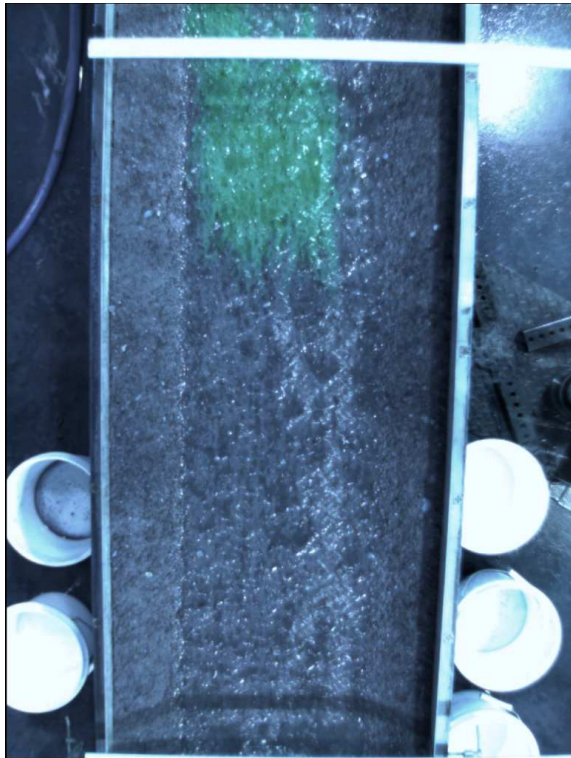

Fig. 16. Flow Velocity Measurement:
Top camera: Shallow surface flow (FDR)

Fig. 17. Flow Velocity Measurement:
Top camera: Channel flow (FDR)

Sediment Concentration

Knowing the discharge, the sediment budget is calculate-able by measuring sediment concentration only. The sampling was performed by means of 1 liter sediment bottles. The sediment bottles were positioned every minute directly at the funnel beyond the outflow geometry of the downstream flume boundary. The bottles were filled with 1 liter of water and sediment suspension and sorted in order of use. By knowing the channel geometry changes in same time resolution (1 minute photo interval) and assuming a mean bulk density of the soil, which was determined with about 1.41 g/cm³, controlling determination of average sediment concentration is available.

The bottle weight of every item was determined just before the experiment runs. After collecting the sediment bottles, the wet weight (bottle + water + sediment) was scaled again. After weighting coagulation liquid was added to the bottles for fasten up the sedimentation process. When the water upon the solid particles in the bottles turned clear, the majority of the water was dumped. Then the bottles were added into the drying oven with oven temperature of 105℃. When all the water was evapor ated, the dry bottles were weight again. Subtracting the dry bottle and sediment weight from the wet bottle and sediment weight, the amount of water is calculate-able. Subtracting the single bottle weight from bottles with dry sediment, the dry sediment mass is calculated. Knowing the temperature of the water, the water weight can be transferred into volume (liter). The sediment concentration of the sample can be determined as follows:

$$Sed_{Conc} = \frac{m_{Sed}}{V_{Water}}$$

[9]

        Sed_{Conc} Sediment Concentration (g/l)
        m_{Sed} Dry Mass of the Sediments (g)
        V_{Water} Volume of Water in the bottles (l)

5.) Results

5.1.) Introduction in Results and Analyses (current stage)

<u>Focus of Current Analyses</u>
Above mentioned data measurements provide a wide range of experiment analyses. The primary focus is on flow hydraulics and the morphology influence on roughness, but as this entire topic relates to soil erosion - outflow sediment concentration data is central issue. Not least, the sediment transport due to gravitational forces of solid particles is impacting flow hydraulics. Not arguing for measuring several available parameters - observation of potential influences might be useful for further analysis and understanding. Concerning the actual rill erosion study, essential impacts are defined by:

- Channel Geometries
- Discharges
- Flow Velocities

For quantifying channel morphology, present stage analyses are based on the more or less stable channel stage conditions. The development of the erosion rills (FDR and SCR) are described as follows:

<u>FDR – Free Developing Rill</u>
The initial situation of the FDR study is the plain levelled and rainfall simulation treated soil body with uniform surface slope of 5.7° respectively y 10%. The soil surface is 1.90 meter long and 0.60 meter wide with 30 degree inclination side rising of 12.5 cm to the metal sheet side boundaries. A central plain soil width of 35 cm remains. This setup was chosen to avoid water flow and erosion directly at the metal sheet borders and to avoid further significant boundary influences or sudden channel boundary breaks.
The soil surface outlet situation was prepared in small half-circular pothole shape of about 10 to 20 cm diameter. This half-circular deepening into the soil surface was shaped as smooth changeover from plain soil surface to the 5 cm deeper positioned downstream boundary of the trapezoid channel outlet.
After preparing and saturation of the soil layer by 2 hours of simulated rainfall (approximately 2.5 cm rainfall depth in 2 hours) and a resting time of the soil of about 1 hour, saturated and free drainage conditions in the upper soil regions were assumed and the experiment was ready to start. The soil preparation caused saturation conditions. Because of this, the surface runoff is less intended to infiltrate because of high matrix potential of dry soils. Another imported effect is the sealing process of the surface by clogging small surface pores with surface runoff washed out particles and raindrop splash. The gravitational compaction of the soil due to rainfall is also of importance to create realistic conditions.

Starting the FDR experiment:
The adjusted water inflow rate into the water reservoir of 0.145 liter per second respectively 0.270 liter per second overflows the reservoir outlet and protection fleece onto the soil surface. A shallow (approximately 1 to 3 mm) water sheet flow covered the soil surface uniformly. The sheet flow intended to increase the average flow velocity of about 20 to 30 cm/s by accumulating into preferential flow paths. These paths might be created either by the panel shape preparation of the surface, small scale path development during the rainfall simulation or by eroding of less resistant particles of the surface by the shallow downstream flow. The water front entering the prepared pothole erodes the rim of the knick point. Due to erosion at the pothole boundary, the circular shape widens and more water intends to enter the pothole at the upstream boundary. Increasing the inflow increases the erosion force. Soon, one or even more channelized inlets from the surface runoff to the pothole develop. Back-cutting erosion occurs, whereas the rim of the plain surface to the channels moves upstream. The shape of the moving knick point remains more or less stable, as the water overflow erodes the rim and transports the soil material into the channel. The material source is transported towards the outlet or accumulated in the channel as a result of equality of erosion forces of the water and resistance forces of the material considering the slope and shape development of the occurring channel.

Directly beyond the knick point, the plunge pool of water overflow scours the steep sloped material as a result of water circulation. Loosening these topographical steps in the soil surface - from plain to channel - sudden breaks in the rim causes further cutting through the material. In the case of multiple channel development during beginning stage of channel erosion, the power of the inflowing water is divided into several rills. Increasing one single rill randomly (by grabbing a preferential flow path, or reaching a weak point in soil structure) this channel arm grabs water majority, because of more use of side inflows which would have been grabbed by other arms otherwise. Grabbing more water causes changes in equilibrium slope in the channel to a less steep rill (water is able to erode more sediment, until the flow velocity by decreasing the slope decreases too). Because of this, the step height at the knick point increases additionally. As a result, even more erosion occurs, the water level at the point of rill concentration decreases, water in other side army fall dry and additional strengthening of channel erosion in the leading channel occurs. Sometimes contrary developments are observed, as the decrease in the water level causes even steeper gradient in the tributary channel system, whereas these side arms grow again temporarily.

However, cutting towards the flume inlet, sooner or later a single main channel develops. Because of the merging system of different side arms, preferential flow path in the surface flow directing the channel creation and coarse as weaker regions in the soil material influence the channel development – as the channel regime itself chooses equilibrium meandering path of flow forces to soil resistance forces and sediment transport situation - a unique but specific channel meandering occurs.

When the back-cutting front finally reaches the upper end to the metal flume reservoir inlet, a sudden bank break occurs because of sudden boundary instability. After eroding and transporting this amount of loose sediment source, the channel begins to stabilise. Less sediment transport is observed, because of the lack of sediment input source to the channel, as the erosion front reached the upper boundary. This situation leads to side bank erosion and scouring erosion at the meander bows, whereas the curve system of the rill develops more straight. Nevertheless, the erosion force of the channel flow decreases also by deep cutting through the sediment body and so a final meander-structure in channel morphology remains. It is assumed, that it is also time related process until slow channel side wall erosion straightens the channel. In fact natural channels receive additional sediment input from above or catchment system, wherewith erosion forces would decrease in average. Because of this, the final morphology might be more stable in nature or even in a longer flume.

Accounting this hypothesis the point of significant reduction and stable stage in sediment concentration considering outflow sampling is assumed to describe more or less stable channel conditions. This stage is the so called equilibrium stage and describes the condition to be compared in the further steps of analyses.
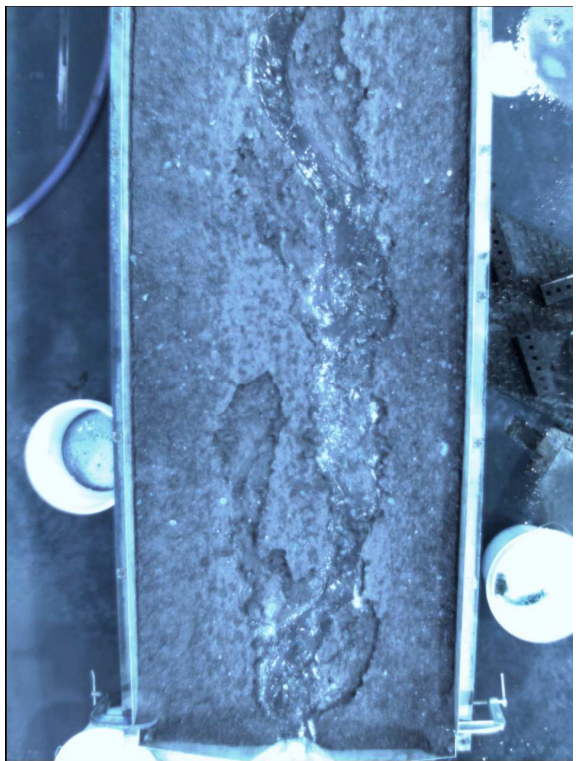
PHOTO SERIES: FDR 0,145 l/s
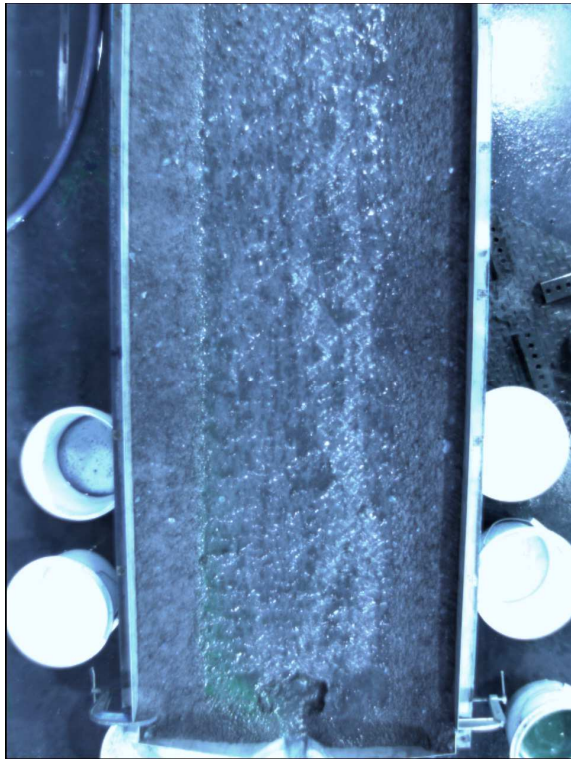
Fig. 18.   Beginning stage of FDR 0,145 l/s:
Shallow surface flow begins pothole scouring
at the downstream flume outlet

Fig. 19.   Two channel arms develop
due to back cut erosion

Fig. 20.   One main channel formats whereas the
Other side arm fells dry

Fig. 21.   Equilibrium channel stage:
The meandering rill is no longer able to
cause significant channel erosion

PHOTO SERIES: FDR 0,270 l/s

Fig. 22. Beginning stage of FDR 0,270 l/s:
the shallow surface flow develops as a deeper
water layer as in the 0,145 l/s experiment

Fig. 23. Only one main channel occurs. The increase
in discharge causes wider initial erosion

Fig. 24. The higher discharge causes less meandering
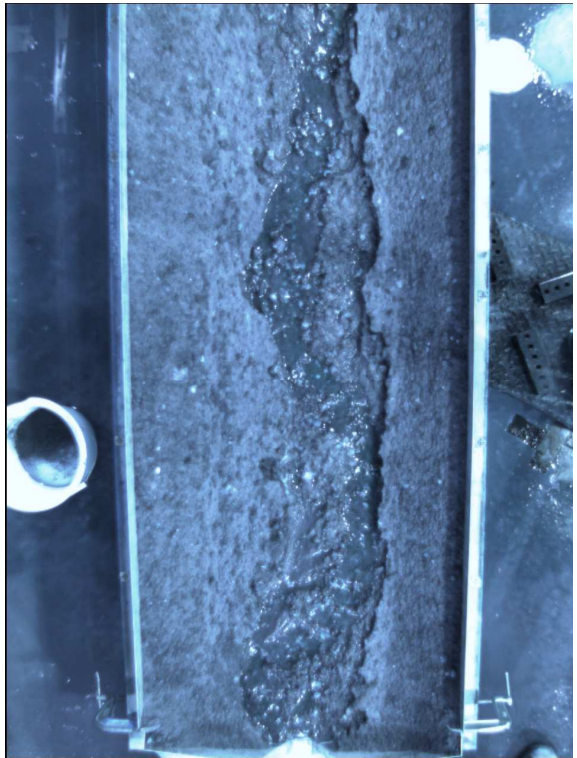**morphology during the FDR**

Fig. 25. Equilibrium channel stage:
The meandering rill shows a smother
characteristic due to increase in discharge

SCR – Straight Constrained Rill

The SCR experiment was developed to produce either a straight channel formation but also an equilibrium stage between erosion and resistance forces. The aim was to induce a beginning stage direction of water flow, whereas the deep scouring and width development of the erosion rill should behave uninfluenced.

The initial situation of the SCR study is the plain and rainfall simulation treated soil body with uniform surface slope of 5.7° respectively 10% with central initial channel. The initial channel was trapezoid shaped with a bottom width of 4 cm, 45 degree side channel boundary inclination and a depth of 4 cm. This geometry is sufficient for concentration of inflow discharges of 0.145 liter per second respectively 0.270 liter per second. Due to initial channel depth of 4 cm and the flume outlet depth of 5 cm below the soil surface at the outlet, there is a 1 cm step from the initial channel bed to the metal outlet boarder. The developing channel undercuts the soil surface inclination wherewith bed formation of the SCR channel increases in the upstream region. After preparation of the initial rill by means of a shape panel, the 1 cm step in soil bed was smoothened out at the metal flume outlet. Then soil preparation by means of rainfall simulation was executed similar to the FDR experiment. Although the soil was threatened in same way by simulated rainfall intensity, because of the initial channel even more surface runoff concentrated in the initial channel and so the channel surface was intended to be threatened more intensively. This may influence the beginning stage of channel formation.

Starting the SDR experiment:

The water inflow rate into the water reservoir was adjusted to 0.145 liter per second respectively 0.270 liter per second as well. The metal reservoir border overflow was protected by textile fleece similar to the FDR experiment.

In contrast to the FDR experiment the flow conditions during the SCR runs were always concentrated. As a consequence, no shallow surface flow is produced in the beginning stage. During the first minutes of the experiment some loose particles at the initial channel surface are transported to the outlet because of the forces of the flowing water. The outlet region was reshaped by the water soon. After eroding the surface unsteadiness the initial channel boundaries resisted to the flow forces and the out flowing water of the flume remained clear. Suddenly channel bed scours occurred whereas these points of unsteadiness acted as knick points for beginning back-cut erosion. The occurrence of these channel bed scours are supposed to result out of small scale erosion of fine materials and the exposition of bigger particles to get flushed out abruptly. Another reason for increase in resistance forces of the soil is in the saturation of the soil ground by the hydraulic pressure conditions in the channel. It is shown in several studies that soil seepage conditions cause significant reduction in soil resistance due to overflow forces. For this reasons weakest point erosions occurs and further bed formation is enabled.

Back-cutting erosion at the scour knick-points created erosion channels into the soil material of the flume. Because of the initial direction of the flow, the deep cutting of the rill is straight in downhill orientation. The deep cutting caused bank breaks at the side boundaries of the channel. Because of no or less meandering of the flow, the water flow velocity was remarkable higher in comparison to the FDR flow. Also the influences of the sidewall to flow direction were lower during the SCR case study. Less turbulences and hydraulic jumps occurred, whereas the energy of the flow had to be dissipated by deep scouring channel erosion. In the end the equilibrium channel inclination was less as it was monitored during FDR runs. This circumstance indicates for different forces acting on creating the equilibrium rill, which is a clear statement for the sensibility of shape roughness.
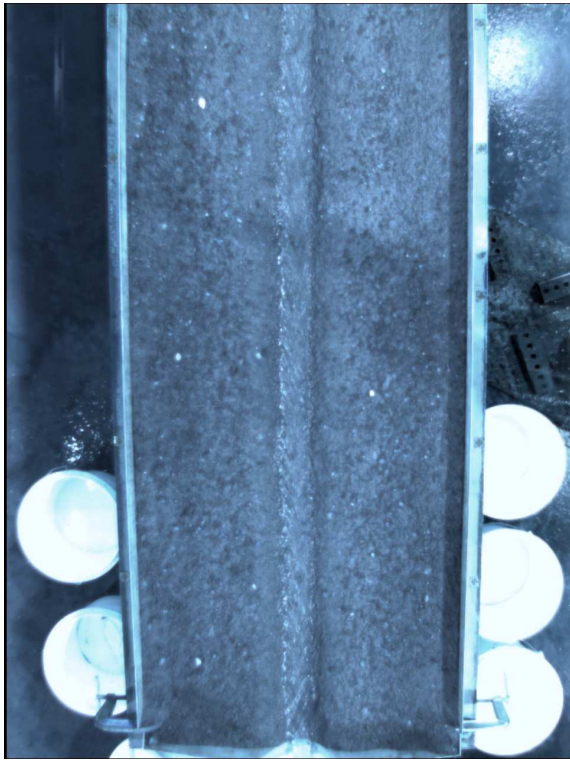
PHOTO SERIES: SCR 0,145 l/s

Fig. 26.   Beginning stage of SCR 0,145 l/s:
The inflow is concentrated in the prepared
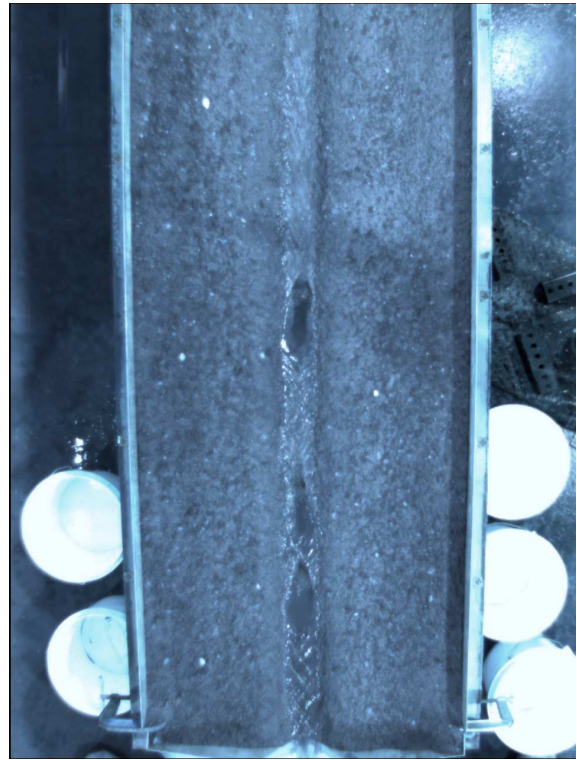**initial rill**

Fig. 27.   "Weakest point" erosion occurs at the channel
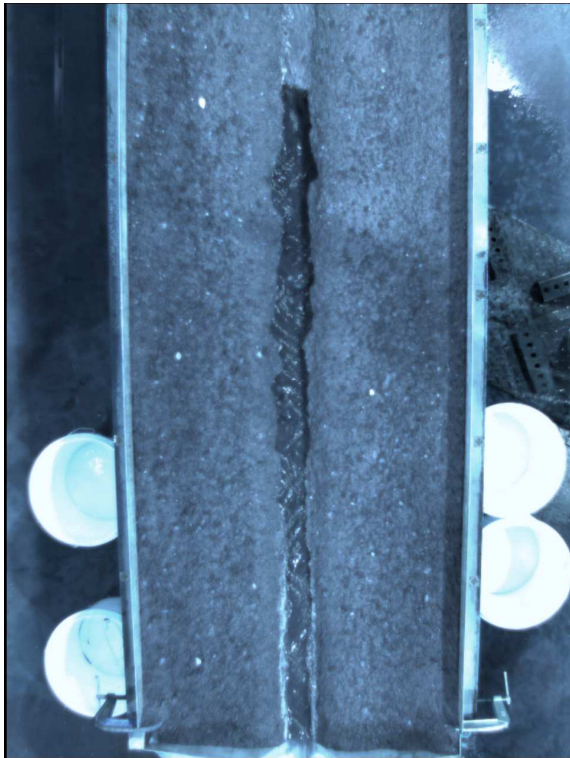**Bed because of regional soil breaks**

Fig. 28.   The scours at the channel bed are starting
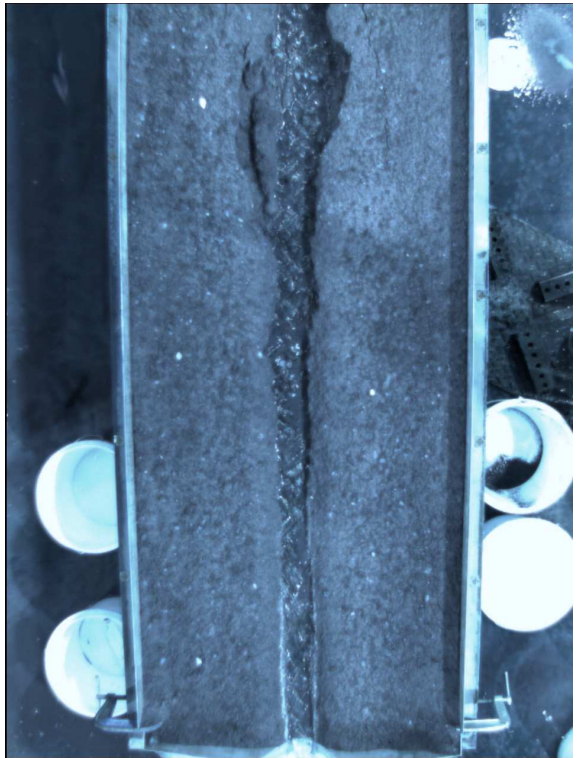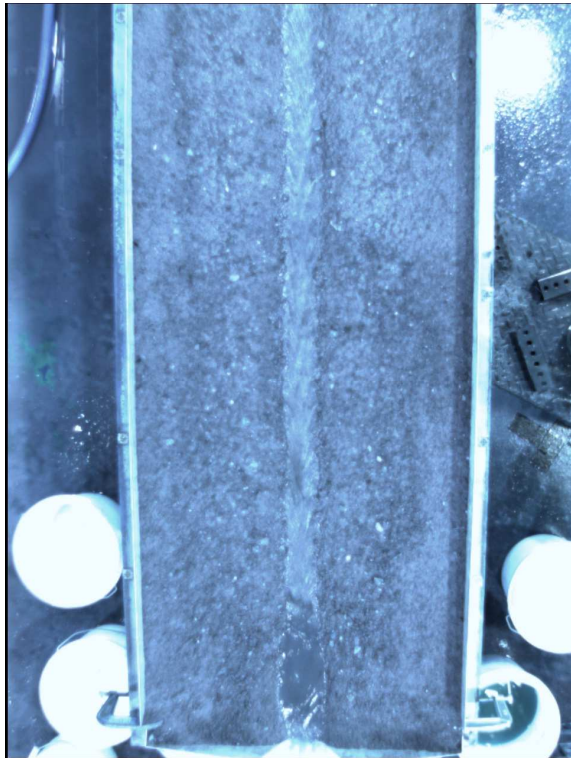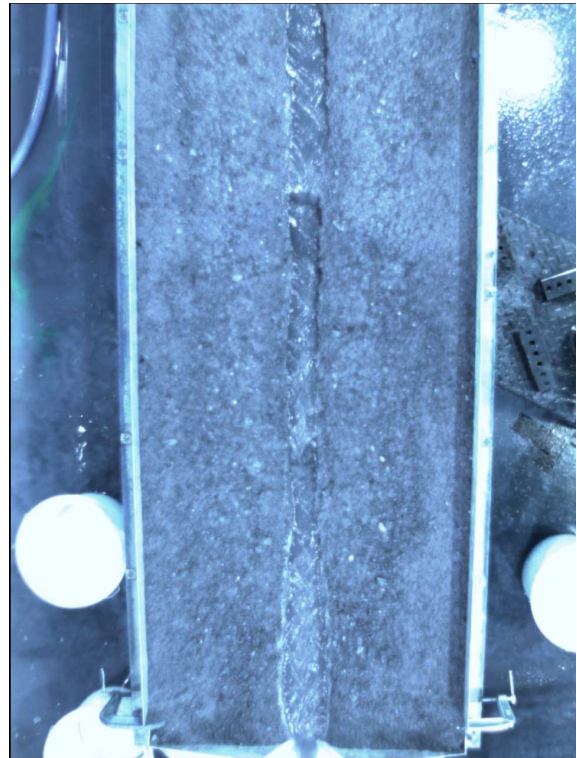**Points of back cut erosion**

Fig. 29.   Equilibrium channel stage:
The channel deepens much more than in the
FDR type. Bank breaks in the deep scouring
Regions at the inlet cause slight shape
unsteadiness

PHOTO SERIES: SCR 0,270 l/s

Fig. 30.   Beginning stage of SCR 0,270 l/s:
The channel depth is higher than in the 0,145 l/s
experiment

Fig. 31.   Quick channel bed erosion and back cutting
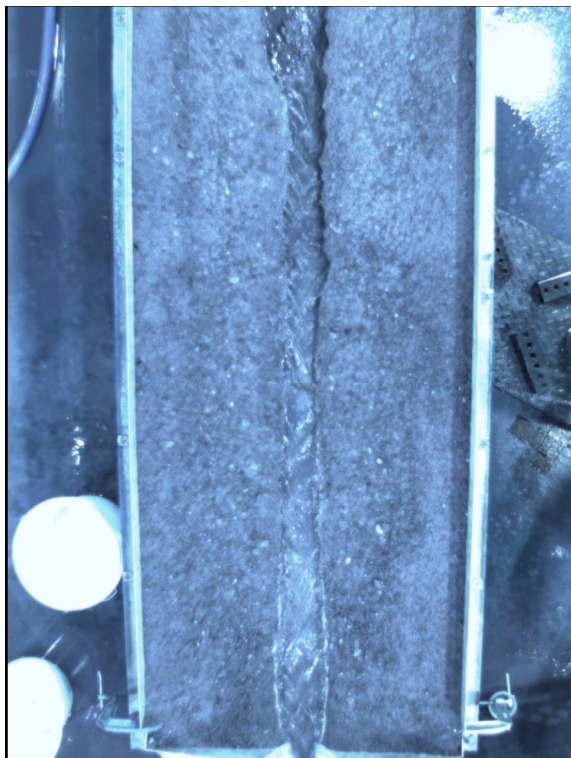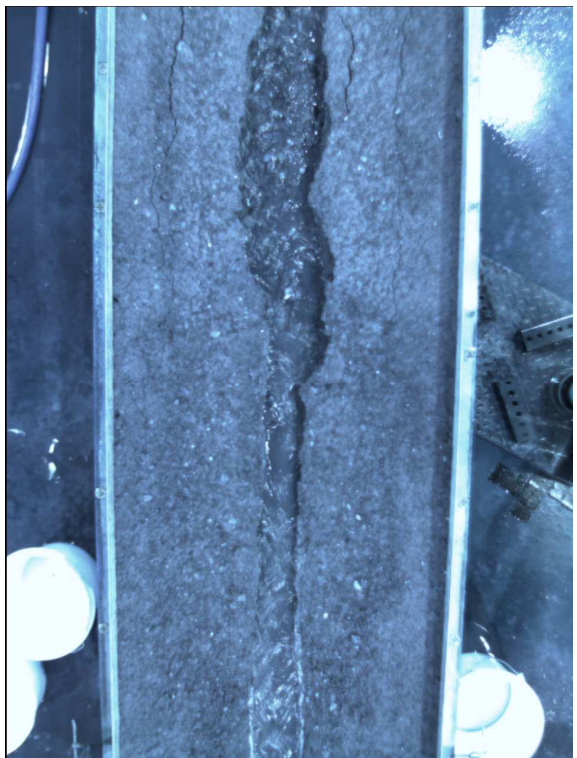**Knick points occur**

Fig. 32.   The channel flow is uniform and straight

Fig. 33.   Equilibrium channel stage:
Bank breaks in the upper regions of the flume
lead to slight channel unsteadiness

25

The calculation of holistic friction roughness caused by skin friction and shape roughness as a sum parameter k_{st} is based on equation [4]:

$$v = k_{st} \cdot R^{2/3} \cdot I^{1/2}$$

[4]

The parameters v (mean channel flow velocity), R (hydraulic radius of the channel) and I (channel inclination) must be defined. The estimation respectively the extraction of these parameters is provided by the rill erosion experiments.

Concretely, the average flow velocity was measured by colour tracer method during all experiments to different stages of channel development. Current analyses concerning the results of velocity measurements for calculating the k_{st} factor are based on equilibrium channel development stage only. The factors R and I are reproduce-able by means of photogrammetric survey of the stereo camera setup as well as manual control measurements. As there are no DEM analyses based on stereo photos for all of the runs up to now, the procedure is to use hand measured channel depth data as well as Microsoft Photoshop analyses of flume images for estimating the channel width and flow path. This procedure is explained in chapter "Photo Analyses (current stage)". The principal behind the photogrammetric analyses is shown in the following chapter:

Photogrammetric Analyses – DEM´s
In general, photogrammetric analyses are based on stereo information of the terrain. Single airborne images of the earth surface provide 2D information only, but analyzing stereo pictures of same content from different point of view interpretation of distance to objects can be extracted in similar way human eyes perform. Therefore several image preparation steps have to be processed (for example: image distortion). After rectifying images from optical distortions special software programs are able to detect comparable points on stereo photo sets. It is essential to determine same objects and points to reproduce height out of the image information.

Following pages illustrate results out of photogrammetric analyses. Input images are photos from the stereo camera setup (about 20 cm distance between camera focus points) at a height of about 2 meters above the flume. The resulting DEM can be used for calculating average channel width and channel bed inclination. The advantage of this procedure is in the distance measure without influencing the experiment and in the possibility of smoothening out of varying point data caused either, by local phenomena or measure failures or local unsteadiness in water surface (hydraulic jumps, e.g.). It is assumed, that smoothened average data represents the flume behaviour more accurate than local point measure. The procedure is illustrated by means of example "Photogrammetric analyzes for FDR" in Fig. 34 to 36 and by the "Photogrammetric analyzes for SCR" in Fig. 37 to 39.

Example DEM
Photogrammetric analyses for FDR

Fig. 34.   Lower stereo photo (FDR)
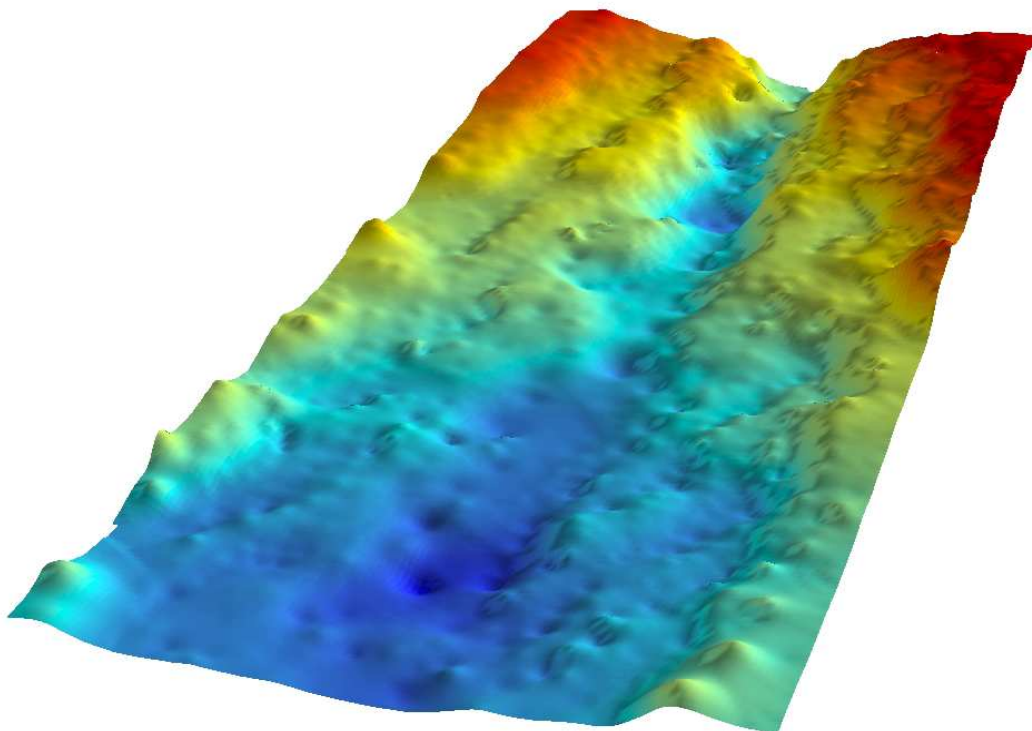

Fig. 35.   Upper stereo photo (FDR)

Fig. 36.   DEM out of FDR data:
Merging the two stereo photos result in
Interpreting height attributes to fitting points

27

Example DEM
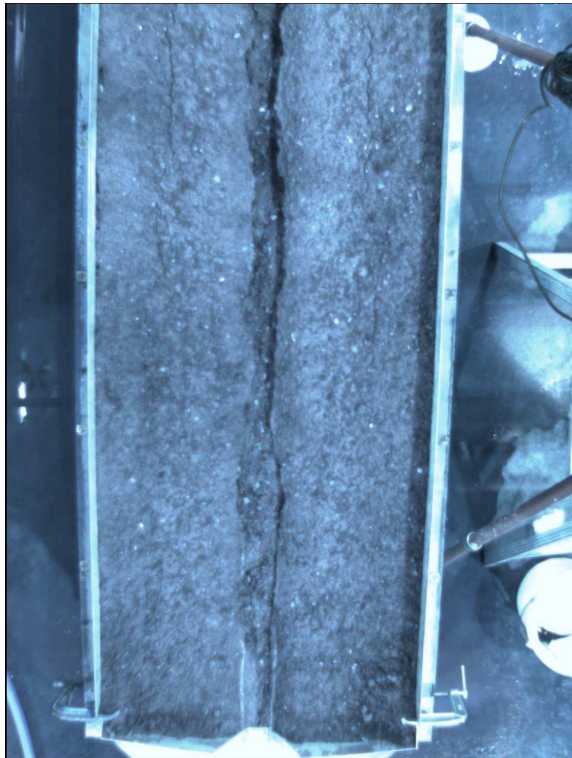Photogrammetric analyses for SCR

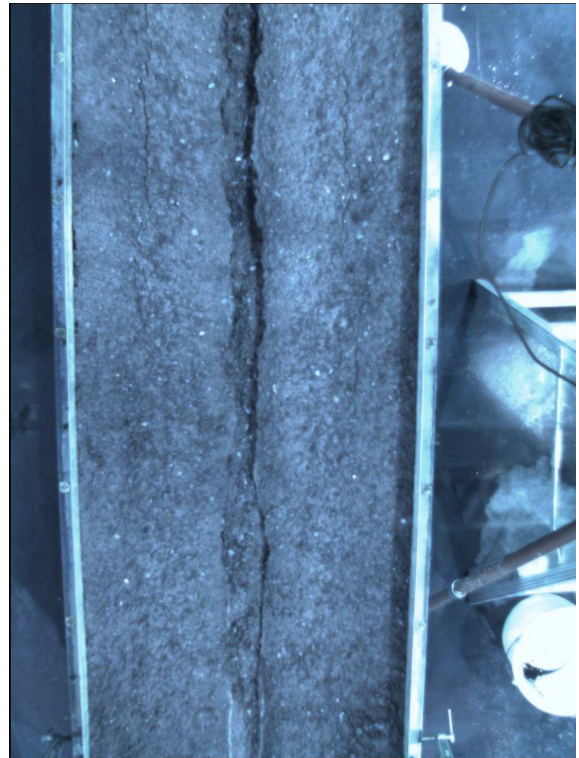**Fig. 37.   Lower stereo photo (SCR)**

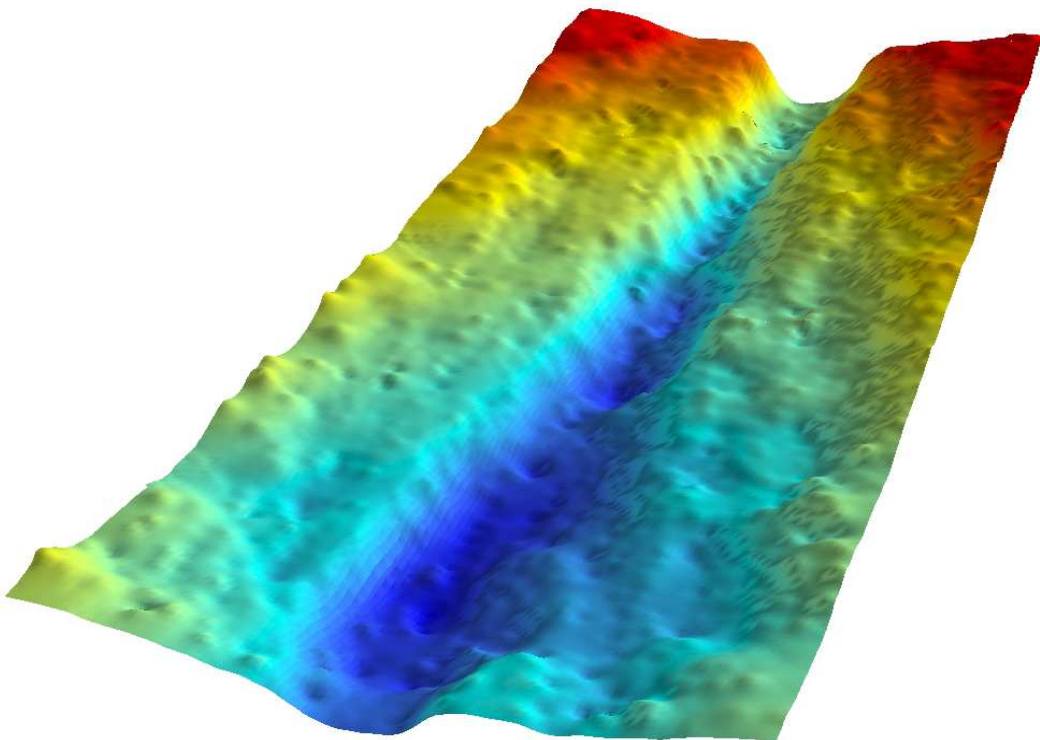**Fig. 38.   Upper stereo photo (SCR)**

Fig. 39.   DEM out of SCR data

28

Image Analyses for Geometry Data (current stage)

As the DEM generation out of stereo photos is not completed yet, the photo analysis is based on single image analysis by means of the Microsoft Photoshop software. The distortions of the pictures were smoothened out by Photoshop software distortion algorithms. By identifying positions of reference points at the flume frame the scale factor of real distances and pixel size can be determined. In this way scaling can be performed and measured distances at the images can be re-calculated as real length.

For estimating channel width three defined cross sections were evaluated and averaged. The three reference widths were taken in the area of stereo photo overlap. One cross section was measured in lower third of flow path, one in the middle section and one width in the upper region.

The definition of flow path is somehow inconclusive: On one hand the definition of the flow path can be assumed different way – for example the symmetric line between the channel boarders or the streamline of highest flow velocity in flow direction e.g. On the other hand some definitions are hardly applicable by having image data only. Flow path definitions might be dispensable concerning large meandering river sections where the river morphology is shaped by very large bows. The streamline definition is also less important in very uniform river regimes with very uniform flow velocity distributions. Considering the narrow flume and the minor possibility for meandering as well as relatively tight turnings in meandering of the erosion rills during the experiment, defining the flow path might be critical point. Changes in "real flow length" are impacting the channel steepness assumptions as well as flow path tortuosity as potential correlation factor for future planned regressions between rill tortuosity and shape roughness. For the actual stage of analyses the flow path length was interpreted by focusing on the waves at the images. The assumed main streamline was drawn with help of Photoshop tools into the referenced pictures. The length of the interpreted streamline was computed by scale transfer due to flume reference points.
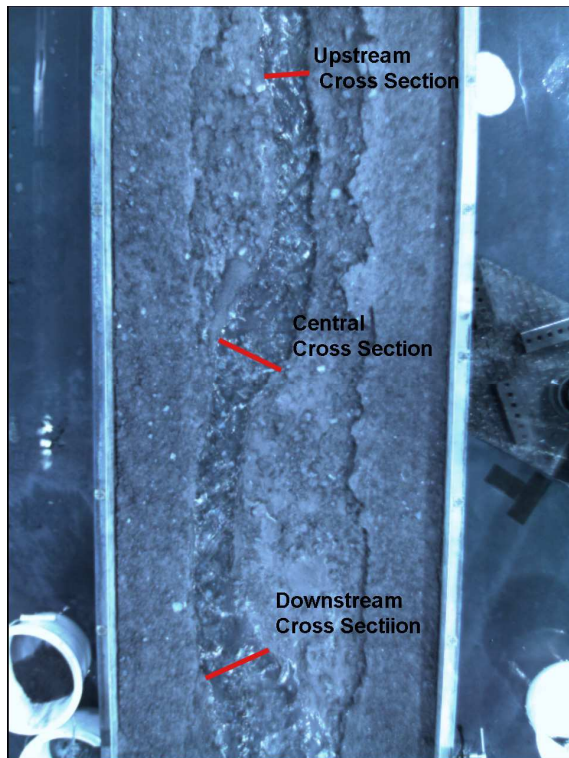

Fig. 40.   Definition of measured cross sections for average channel width estimation
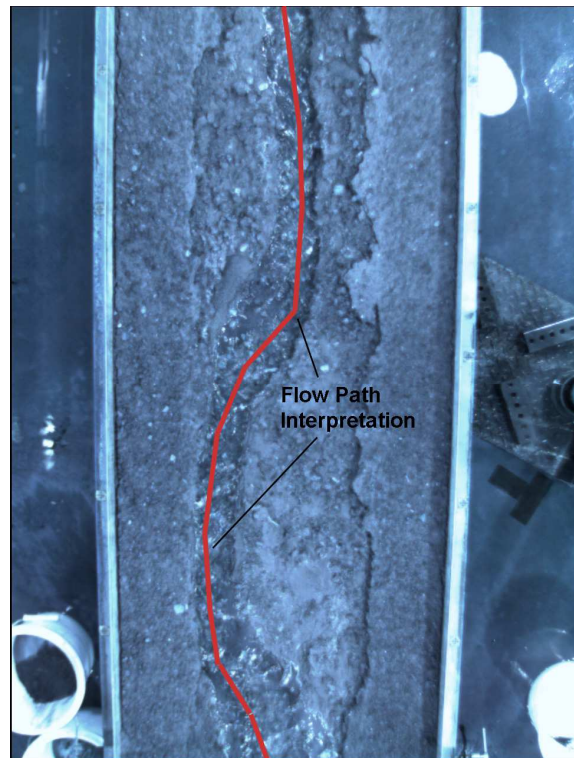
Fig. 41.   Interpretation of the flow path For channel length and tortuosity estimations

<u>Analyzing Techniques</u>

The overall analyzing technique as mentioned in the above chapters is the extraction of the global roughness factor k_{st}, implemented in the *Gauckler-Manning-Strickler* equation [4]. As further mentioned, the average channel flow velocity *v* was determined by colour tracer measures in an adequate way.

The channel inclination *I* can be derived by photo analyses – either by analyzing DEM computations due to stereo photogrammetric procedures or: Knowing the surface inclination of the soil (10% or 5.7°) considering the channel depth at inlet and outlet (manual hand measures) and estimating the real streamline length (Photoshop software). Thus, a re-calculation of the inclination is enabled. This procedure was chosen as source for further analyses.

The hydraulic radius *R* is defined as relation of the cross sectional area *A* and the wetted perimeter *U* of the channel:

$$R = A / U \qquad\qquad [10]$$

For calculating *R* the real respectively the average channel cross sectional geometry has to be defined. In fact: as the *Gauckler-Manning-Strickler* equation [4] is valid for steady state flow and more or less uniform flow conditions only, these conditions should be fulfilled anyhow. But: As mentioned in the beginning of the experimental idea this is not the case because of lack of knowledge concerning developing rill morphology. This circumstance is exactly the point of interest of this study. A variety of hypothesis and agreements have to be defined to use equations and relations adequately. Especially the *Gauckler-Manning-Strickler* equation [4] seems to behave sensitive to violations of defined user conditions. However, equation [4] is widely used in surface erosion models as well. The task is: How significant are violations onto this hypothesis and are the further conclusions to get out of present observations? A satisfying experiment output could be the predictability of uncertainty concerning hypothesis [4] respectively to describe relations between violations in uniformity and the influence onto total roughness assumptions – due to channel morphology.

However, to handle the hardly determinable parameter *R* the decision was to estimate different realistic channel shapes considering the measured average channel widths. For this reason, two types of possible channel geometry were investigated: a triangular and a rectangular shape:
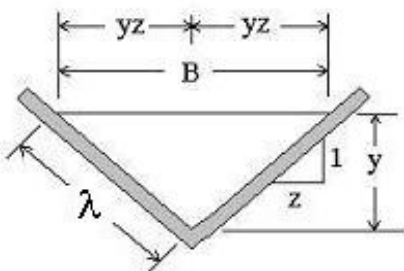
Fig. 42.   **Triangular shape of the channel**   Fig. 43.   **Rectangular shape of the channel**
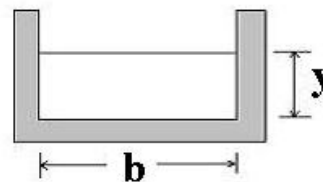
This cross sectional geometry assumptions are neither naturally or realistic for sure. Despite this, the triangular shape describes a very deep shaped (considering flow depth and the bed channel shear stress) cross section as well as the rectangular describes the shallowest continuous channel shape.

Not knowing the channel shape exactly assuming different cross sectional geometries for covering upper and lower but feasible conditions will end up with computing two values for

every relation. In this way, a specific range of realistic estimations will be the result. Assuming the natural channel geometries R value will be covered by this range. As a single value to compare different runs, the mean value between upper and lower assumption is illustrated (chapter: 5.3).

Based on the law of continuity of mass the relation between discharge q, mean flow velocity v and average cross sectional area A is described as follows:

$$q = A \cdot v \qquad [11]$$

As q is known respectively can be estimated as average of inflow rate (q_1=0.145 l/s and q_2=0.270 l/s) and the measured outflow every 5 minutes and v is measured by colour tracer method, A can be derived. Assuming triangular and rectangular channel cross section geometries as mentioned above (Fig. 42 and Fig. 43), following equations [12] to [19] can be used to calculate R out of A and the averaged channel width (Photoshop software):

Triangular Shape Assumption (Fig. 42):

$$A_{tri} = \frac{B \cdot y}{2} \qquad [12]$$

y:

$$y = \frac{2 q_{mean}}{v_{mean} \cdot B} \qquad [13]$$

U and *R*:

$$U_{tri} = 2 \cdot \left(\sqrt{\left(\frac{B}{2} \right)^2 + y^2} \right) \qquad [14]$$

$$R_{tri} = \frac{B \cdot y}{4 \cdot \left(\sqrt{\left(\frac{B}{2} \right)^2 + y^2} \right)} \qquad [15]$$

Rectangular Shape Assumption (Fig. 43):

$$A_{rec} = b \cdot y \qquad [16]$$

y:

$$y = \frac{q}{v \cdot b} \qquad [17]$$

$$U_{rec} = 2y + b \qquad [18]$$

$$R_{rec} = \frac{(b \cdot y)}{(2y + b)}$$

[19]

The above mentioned procedure to calculate the parameters R and I leads to estimations of the k_{st} factors. The result of this inverse procedure for determining calibration factor k_{st} contains information about the range of the roughness value. As the soil, discharge and flume conditions are held constant during the experimental sets (q_1=0.145 l/s; q_2=0.270 l/s) differences in between the calculated roughness factors considering *Gauckler-Manning-Strickler* equation [4] are assumed to be based in shape roughness influences.

In further step, reasons for the behaviour in roughness impacts shall be discussed. Possible relations and regressions of influencing parameters shall be tested. In this way it might be enabled to understand global roughness and to explain shape roughness fractions more explicitly. At this point of research of the "Experimental Rill Erosion Development Study" no regression analyses were performed. Future case studies will concentrate on explanation of results, whereas the present stage is discussion basis if there is significance in shape depending roughness impact generally. However, for the case of remarkable potential in shape roughness influence, some additional calculations to the channel flow conditions have been done. The results and analyses are shown in following chapters 5.2 and 5.3. Concerning supposed relations of impact further studies might indicate regression able parameters explained following:

Possible Indicators for Shape Roughness Explanation

Tortuosity

The tortuosity of a path is defined as follows:

$$T = \frac{L}{X}$$

[20]

The tortuosity describes the relation between the real path lengths (streamline length) and the shortest theoretical path length (direct connection).
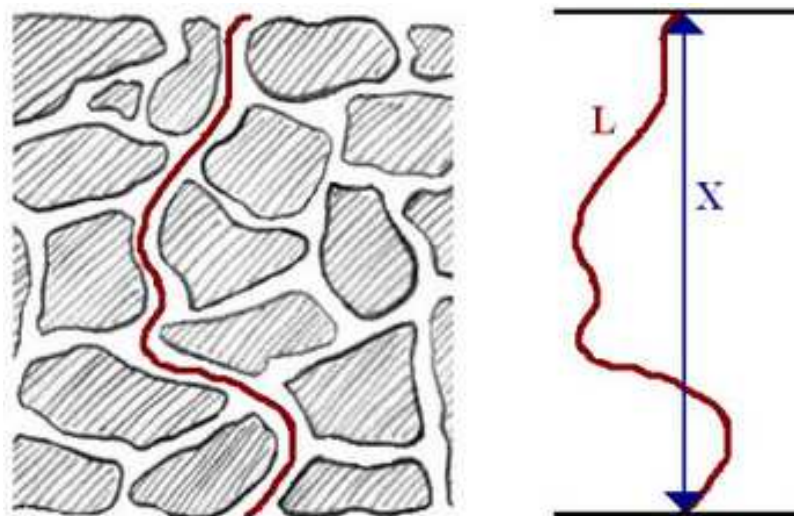

Fig. 44. **Explanation of tortuosity; Source:**
Factors that affect mass transport from drug eluting stents into the artery
wall by B. O'Connell, T. McGloughlin, M. Walsh, 2010

Tortuosity is not accounting for the number or steepness of turnings. Force and momentum relating laws might not be explainable by this single factor adequately. However, as tortuosity is easy measurable factor and is describing some length behaviour of a turning path, possible relations shall be tested. At least for calculating the real flow path length tortuosity is important value.

Froude Number

The *Froude Number* is defined as follows:

$$Fr = \frac{v}{\sqrt{g \cdot L}}$$

[21]

Where *Fr* is the dimensionless *Froude Number*, *v* the velocity, *g* is the gravitational force, and *L* is a specific length – particularly the flow depth. The *Froude Number* describes the relation between inertia forces of the flow and gravitational forces. If the dimensionless *Froude Number* exceeds the value of 1.0 supercritical flow occurs whereas disturbances in flow have no effect on upstream flow. The change from under critical flow condition to supercritical flow condition develops continuously and is not detectable by eye. The change from supercritical to under critical conditions appears locally and is visible as the so called "hydraulic jump" phenomena. Energy of the flowing water gets dissipated. Repeatedly changes in flow conditions result in significant energy dissipation.

Reynolds Number

The *Reynolds Number* is defined as follows:

$$\text{Re} = \frac{v \cdot L}{\nu}$$

[22]

Where *Re* is the dimensionless *Reynolds Number*, *v* the velocity, *L* is a specific length – particularly the flow depth and ν is the kinematic viscosity. The *Reynolds Number* describes the relation between inertia forces of the flow and friction forces. The dimensionless number points out the turbulence conditions in the fluid – from laminar to turbulent flow. Depending on the turbulence of flow, boundary friction is of different impact.

5.2.) Experimental Data Summary

*Up to now, the experiment data is analysed incompletely!*

Thus, the following pages illustrate the actual stage of analyses whereas later publications may change in content and conclusions slightly. As the model measurements were adopted during the experiments, initial and incomplete runs were repeated afterwards. Nevertheless, the following results show the trend of results and analyses.

Experimentally measured Data
The measurements of the 12 (2 types: FDR, SCR, 2 discharges, 3 replications) runs show similar behaviour based on run type (FDR, SCR). Because of this data output of every combination of type and discharge is illustrated exemplarily.

The first graph of every set-up illustrates the outflow discharge measurements in liter per second (Outflow), executed in minute 1, 2, 5 and every following 5 minute interval of the model run. The Infiltration in liter per second is indirect measurement and is extracted by knowing the continuous model inflow discharge (0.145 l7s respectively 0.270 l/s) and the measured model outflow. The infiltration is the difference of the model inflow and outflow. The second graph shows the measured Sediment Concentration in grams per liter. The Sediment Concentration data was measured in one minute interval. The rill development graph (graph 3) illustrates the channel length (Rill Length) and the Rill Depth. This analysis was undertaken manually every 5 minutes. The fourth graph of every run shows the flow velocity data. Therefore, every 5 minutes the channel flow velocity, respectively the shallow surface flow velocity during the early FDR stage was measured by colour tracer method. The blue illustrated points of the FDR runs show the shallow surface flow velocities whereas the red coloured points in the graph illustrate the channel flow velocities.

EXPERIMENTAL RUN: FDR 0,145 l/s

Outflow / Infiltration

Sed.Conc.

Rill Development
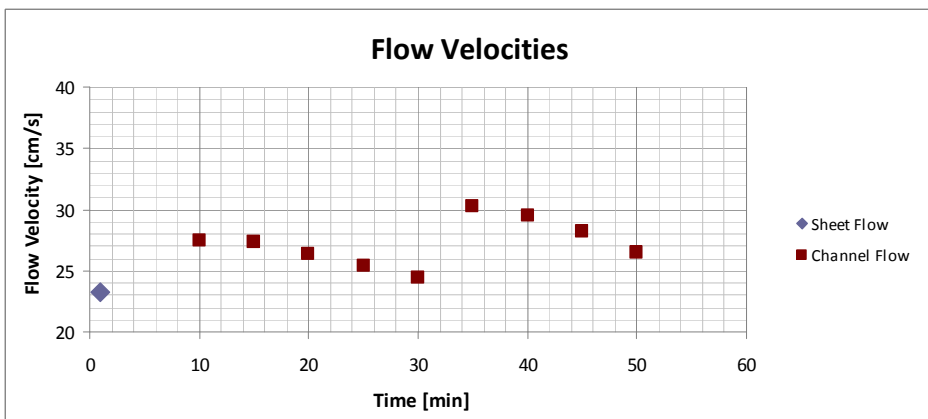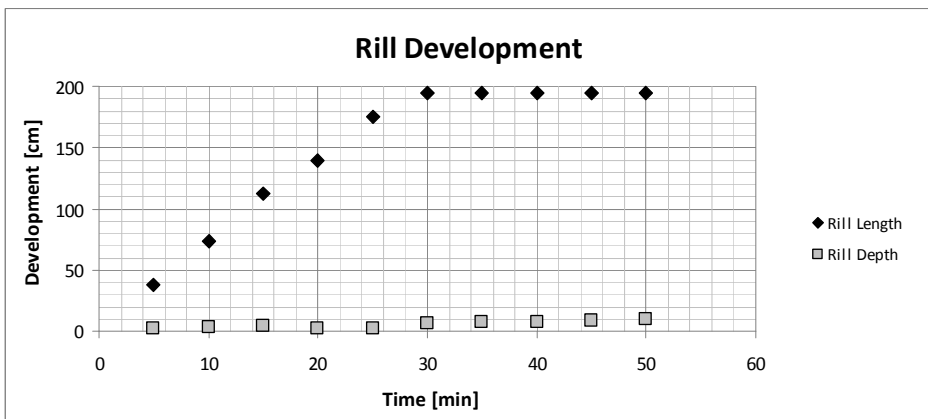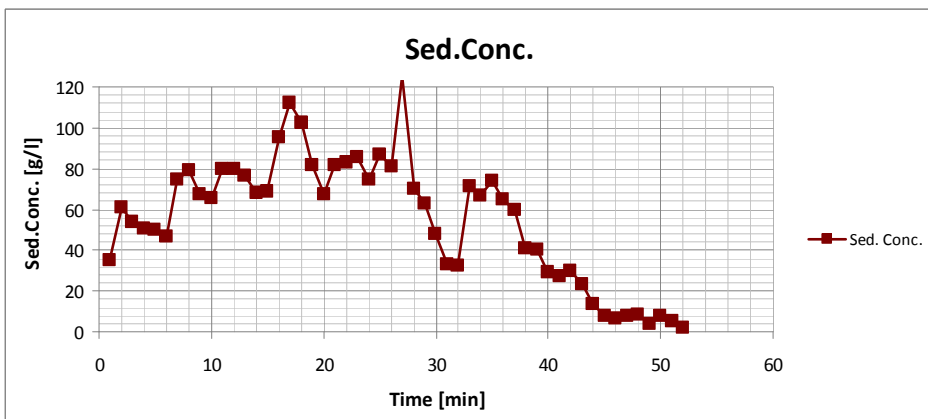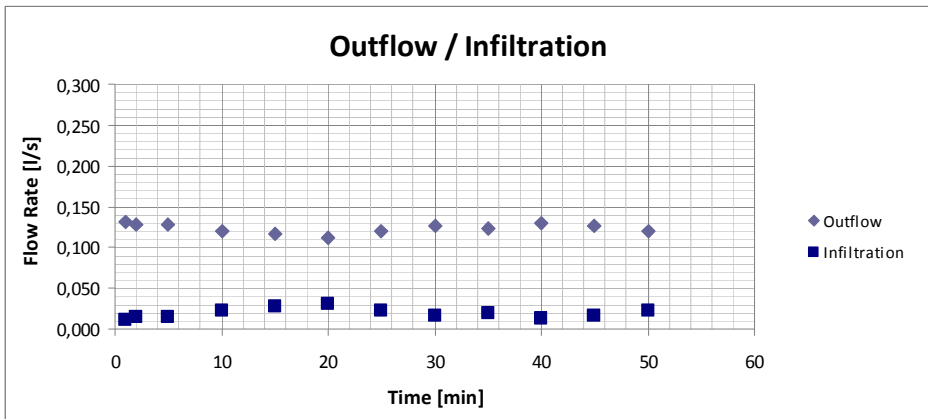
Flow Velocities

Graph 4-7   **Outflow/Infiltration, Sediment Concentration, Rill Development and
Flow Velocities for the run: FDR 0,145 l/s**

35

EXPERIMENTAL RUN: FDR 0,270 l/s

Outflow / Infiltration

Sed.Conc.

Rill Development
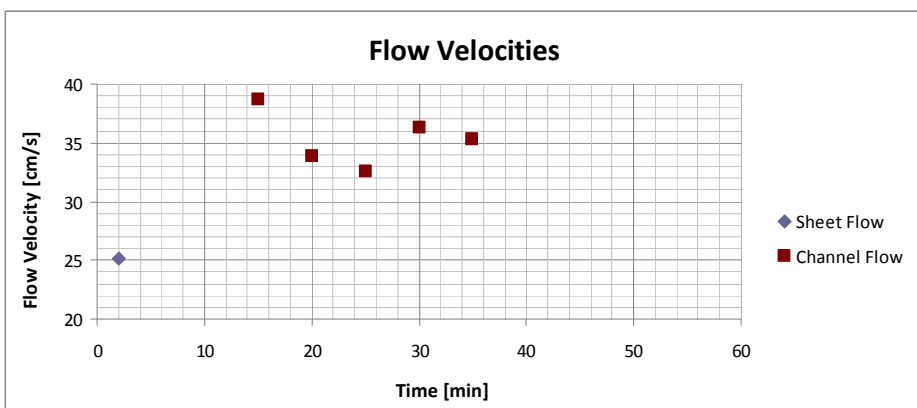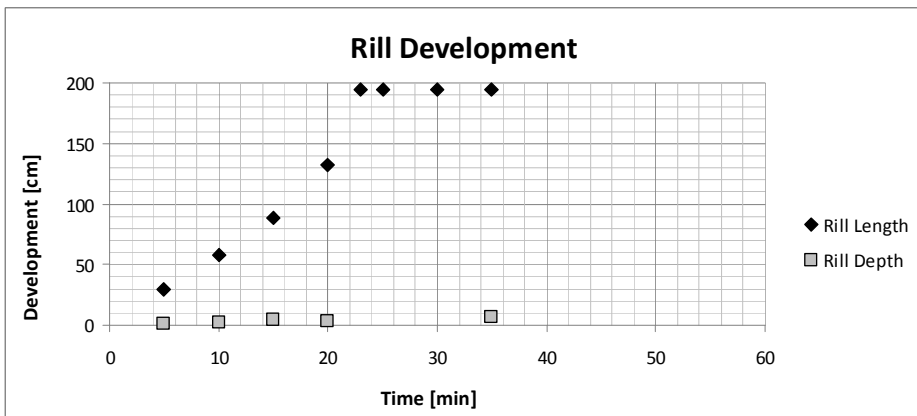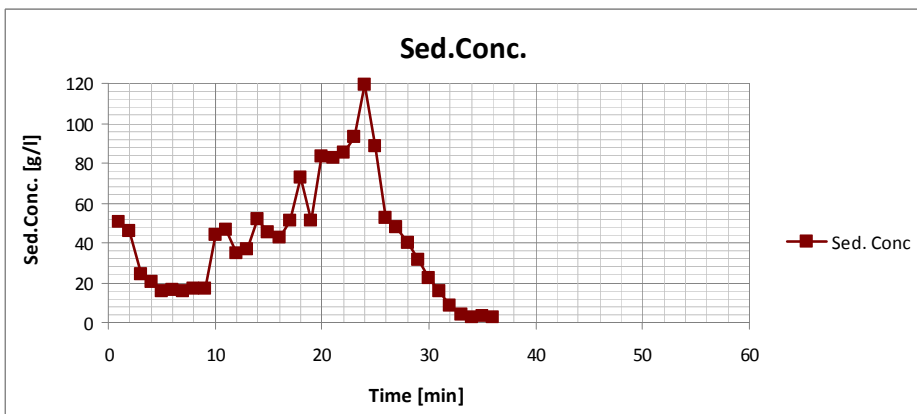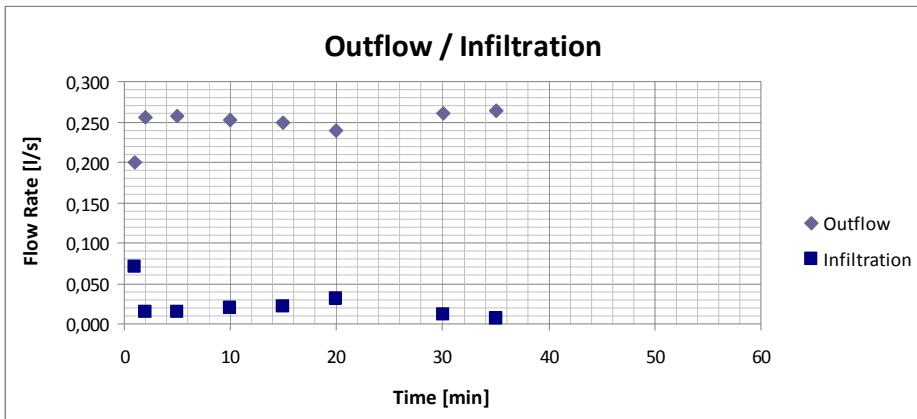
Flow Velocities

Graph 8-11   Outflow/Infiltration, Sediment Concentration, Rill Development and
Flow Velocities for the run: FDR 0,270 l/s

EXPERIMENTAL RUN: SCR 0,145 l/s

Outflow / Infiltration

Flow Rate [l/s] vs Time [min]

Legend: ◆ Outflow, ■ Infiltration

Sed.Conc.

Sed.Conc. [g/l] vs Time [min]

Legend: ■ Sed. Conc.

Rill Development

Development [cm] vs Time [min]

Legend: ◆ Rill Length, ▢ Rill Depth

Flow Velocities

Flow Velocity [cm/s] vs Time [min]

Legend: ■ Channel Flow

Graph 12-15   Outflow/Infiltration, Sediment Concentration, Rill Development and Flow Velocities for the run: SCR 0,145 l/s

EXPERIMENTAL RUN: SCR 0,270 l/s

Outflow / Infiltration

- Outflow
- Infiltration

Sed.Conc.

- Sed. Conc.

Rill Development

- Rill Lemgth
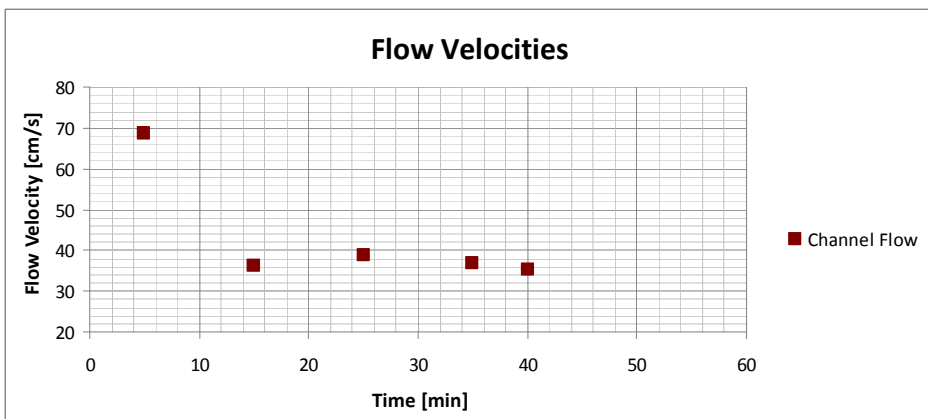- Rill Depth

Flow Velocities
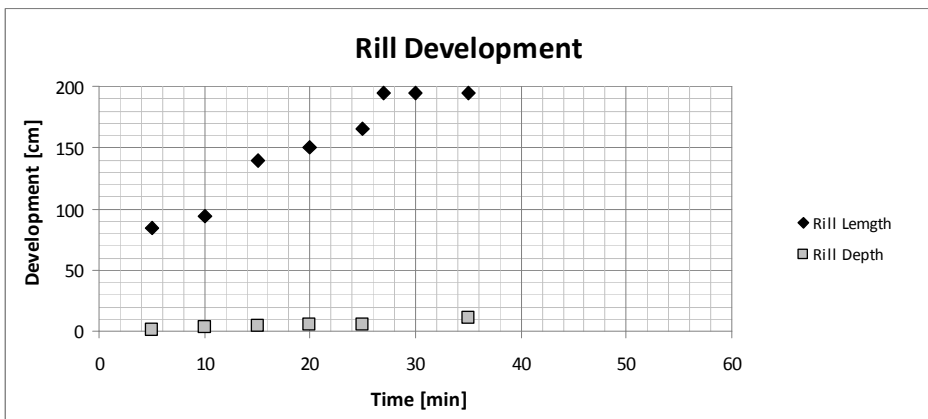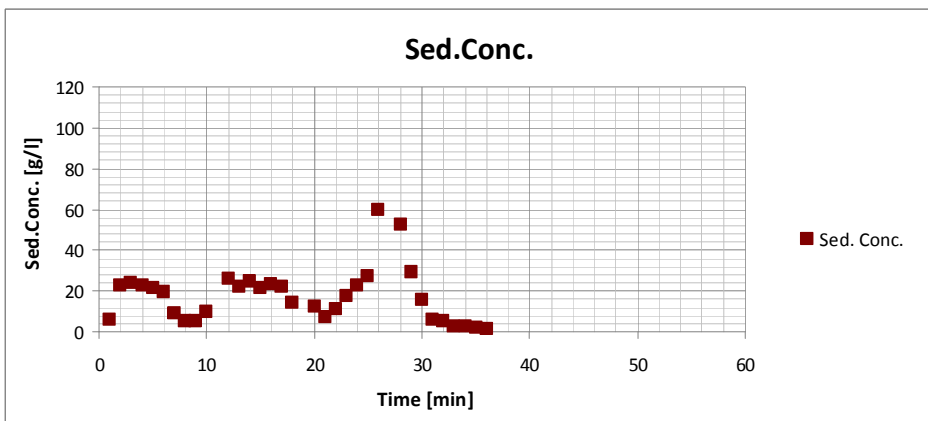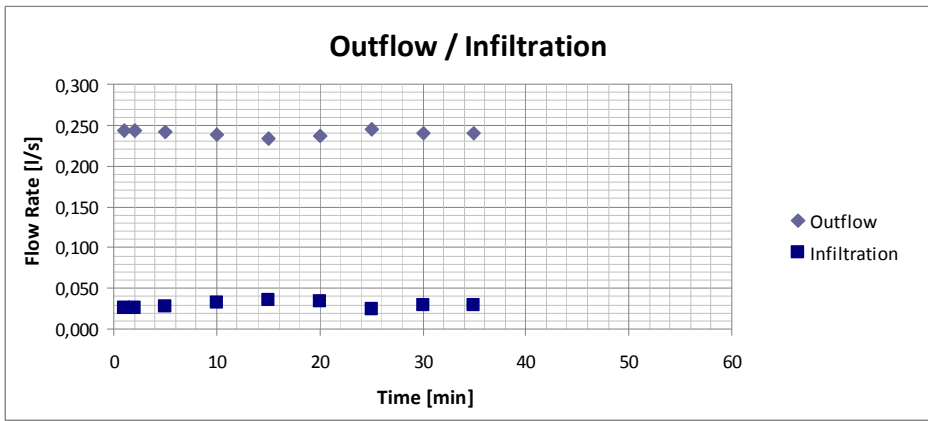
- Channel Flow

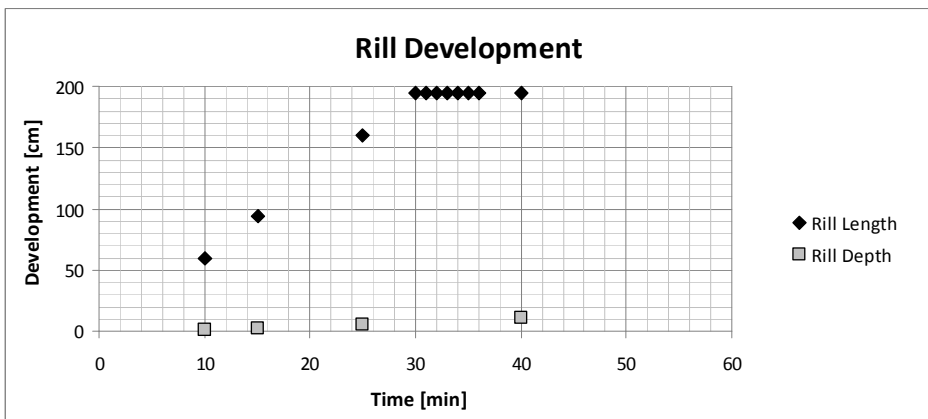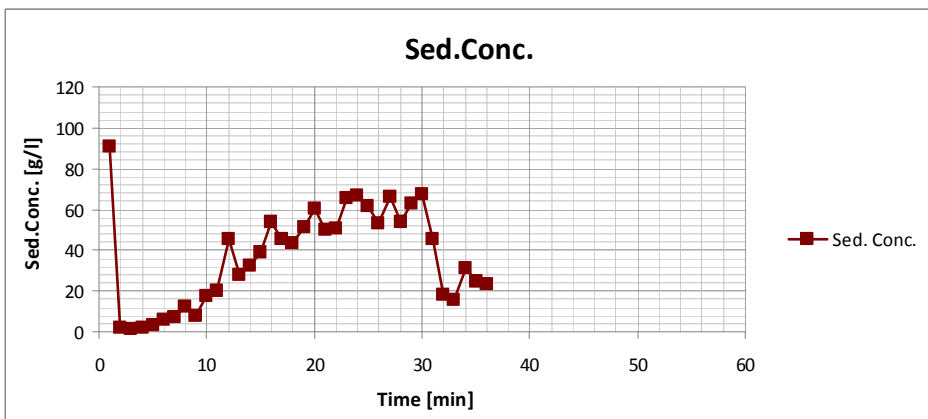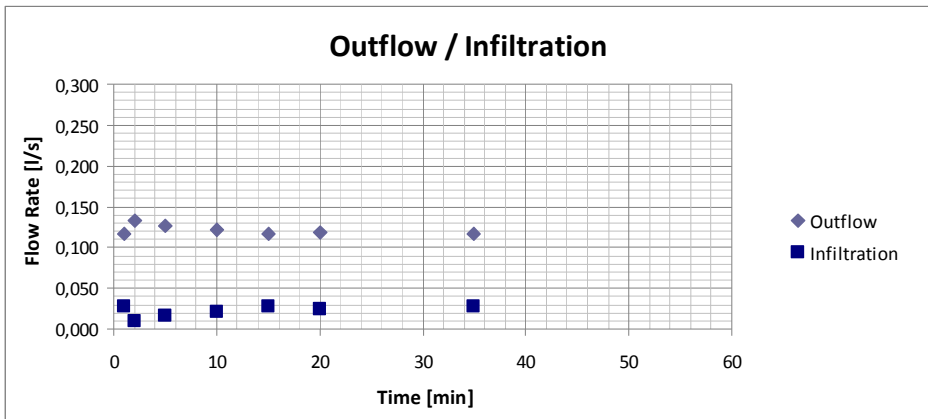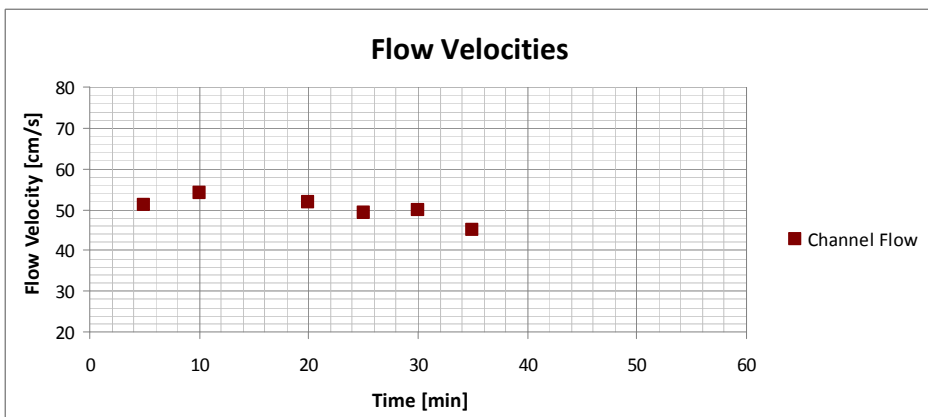**Graph 16-19   Outflow/Infiltration, Sediment Concentration, Rill Development and Flow Velocities for the run: SCR 0,270 l/s**

Data Summary

Run Nr.	Type	Measurments				
		v mean	Q mean	Channel Width	Channel Slope	Channel Tortuosity
		cm/s	l/s	cm	cm/cm	cm/cm
1	FDR11	27	0,130	8,0	0,100	1,048
2	SCR11	30	0,132	8,4	0,080	1,000
3	FDR12	26	0,130	9,5	0,100	1,028
4	SCR12	35	0,131	7,9	0,080	1,000
6	SCR13	26	0,140	9,2	0,080	1,000
7	SCR21	33	0,253	9,0	0,070	1,000
8	FDR21	27	0,255	9,2	0,080	1,062
9	SCR22	41	0,260	8,8	0,095	1,000
10	FDR22	25	0,255	9,5	0,090	1,097
11	SCR23	35	0,259	9,0	0,075	1,000
12	FDR22	31	0,266	9,0	0,090	1,055

Tab. 1. **Summary of measured data: v (velocity) mean, Q (discharge) mean, Channel width, Channel slope, Channel Tortousity**

5.3.) Analyses

Table 1 shows results of direct experiment measurements, simple estimations of flow velocity data based on colour tracer method and data extraction out of top view photo analysis concerning channel slope and channel tortousity values. By means of above illustrated and listed measurements (Tab. 1), the *Manning-Strickler-Factores*, based on equation [4]:

$$v = k_{st} \cdot R^{2/3} \cdot I^{1/2}$$ [4]

were calculated. Accounting for triangular and rectangular channel cross sectional geometry assumptions (Tab.2), the corresponding k_{Str} (*Manning-Strickler-Factor*) are listed in Table 3. In addition, the digitized flow path length and channel width out of stereo camera data were implemented into the calculations. The extracted k_{Str} factors (Tab. 3) are compared to common *Manning-Strickler* values, used in river engineering.

Run Nr.	Type	Valocity and Channel Geometrics			
		v mean (*)	Area Cross Sec.	Wet Perimeter Triangle	Wet Perimeter Rectangular
		cm/s	cm²	cm	cm
1	FDR11	28	4,8	8,4	9,2
2	SCR11	30	4,5	8,7	9,5
3	FDR12	27	5,0	9,8	10,6
4	SCR12	35	3,7	8,1	8,8
6	SCR13	26	5,4	9,5	10,3
7	SCR21	33	7,6	9,6	10,7
8	FDR21	28	9,5	10,1	11,2
9	SCR22	41	6,3	9,3	10,3
10	FDR22	27	10,2	10,4	11,7
11	SCR23	35	7,3	9,6	10,6
12	FDR22	33	8,6	9,8	10,9

Tab. 2. Summary of calculated data: v (*) (velocity) mean with accounted tortuosity (Tab. 1), Area of the Cross Section, Perimeter of triangular cross section, Perimeter of rectangular cross section

Run Nr.	Type	Manning-Strickler-Factors			
		k_{Str} Triangle	k_{Str} Rectangular	$k_{Str\,(*)}$ Triangle	$k_{Str\,(*)}$ Rectangular
		$m^{1/3}/s$	$m^{1/3}/s$	$m^{1/3}/s$	$m^{1/3}/s$
1	FDR11	27	28	28	30
2	SCR11	35	37	-	-
3	FDR12	27	29	28	30
4	SCR12	45	48	-	-
6	SCR13	29	31	-	-
7	SCR21	32	34	-	-
8	FDR21	21	23	22	24
9	SCR22	37	39	-	-
10	FDR22	18	20	20	21
11	SCR23	33	36	-	-
12	FDR22	24	26	26	28

Tab. 3. Summary of extracted factors out of the model experiment: k_{Str} is the Manning-Strickler-Factor based on the experiment measurements (without accounting for channel tortuosity in the experiment measurements (without accounting for channel tortuosity in FDR runs); k_{Str} is the k_{Str} is the Manning-Strickler-Factor, accounting for tourtosiyt channel lengthening.

| Run Nr.	Type	Froude and Reynolds Numbers			
		Froude Triangle	Froude Rectangular	Reynolds Triangle	Reynolds Rectangular
		-	-	-	-
1	FDR11	0,8	1,1	3,1E+03	1,5E+03
2	SCR11	0,9	1,3	2,9E+03	1,5E+03
3	FDR12	0,8	1,1	2,6E+03	1,3E+03
4	SCR12	1,2	1,6	3,1E+03	1,6E+03
6	SCR13	0,8	1,1	2,9E+03	1,4E+03
7	SCR21	0,8	1,2	5,3E+03	2,6E+03
8	FDR21	0,6	0,8	5,2E+03	2,6E+03
9	SCR22	1,1	1,5	5,5E+03	2,8E+03
10	FDR22	0,5	0,8	5,0E+03	2,5E+03
11	SCR23	0,9	1,2	5,4E+03	2,7E+03
12	FDR22	0,7	1,0	5,6E+03	2,8E+03

Tab. 4. Summary of extracted factors out of the model experiment: k_{Str} is the Manning-Strickler-Factor based on the experiment measurements (without accounting for channel tortuosity in the experiment measurements (without accounting for channel tortuosity in FDR runs); k_{Str} is the k_{Str} is the Manning-Strickler-Factor, accounting for tourtosiyt channel lengthening.

Tables 2, 3 and 4 illustrate the main focus of the present erosion channel analyses. Table 2 shows channel velocity and channel geometry and illustrates estimated parameters for the k_{Str} (*Manning-Strickler-Factor*) calculation. Therefore tortuosity from top view photo analysis was taken into account concerning mean flow velocity calculation. Based on channel width photo analysis, flow velocity and discharge measurements, the relating channel depth and cross sectional area was calculated referring to triangular respectively rectangular channel cross section assumptions. Table 3 shows the *Manning-Strickler-Factor* calculation based on equation [4]. The Table 3 is fractioned into *Manning-Strickler-Factors* with and without accounting for channel tortuosity to understand the channel morphology influence of flow path length only. The values of the k_{Str} factor are slightly changing due to triangular and rectangular channel cross section assumptions because of the difference in the hydraulic radius R:

$$R = A/U$$ [10]

In this way, the calculated k_{Str} factors for triangular cross sections is slightly lower than for rectangular cross sections because of less (assumed) channel boundary, which causes same frictions based on *Gauckler-Manning-Strickler* hypothesis. Additionally, table 4 shows calculated and dimensionless Froude and Reynolds numbers based on channel geometrics and flow velocity measurements. In general, SCR runs intend to cause higher *Froude Numbers* and also slightly higher values of *Reynolds Numbers*. Possible reasons for the illustrated trends in k_{Str}, *Froude* and *Reynolds Numbers* are discussed in the following chapter (Conclusions). A graphical overview to the k_{Str} model experiment output is shown in the following Graphs 20 and 21.

Manning-Strickler-Factors
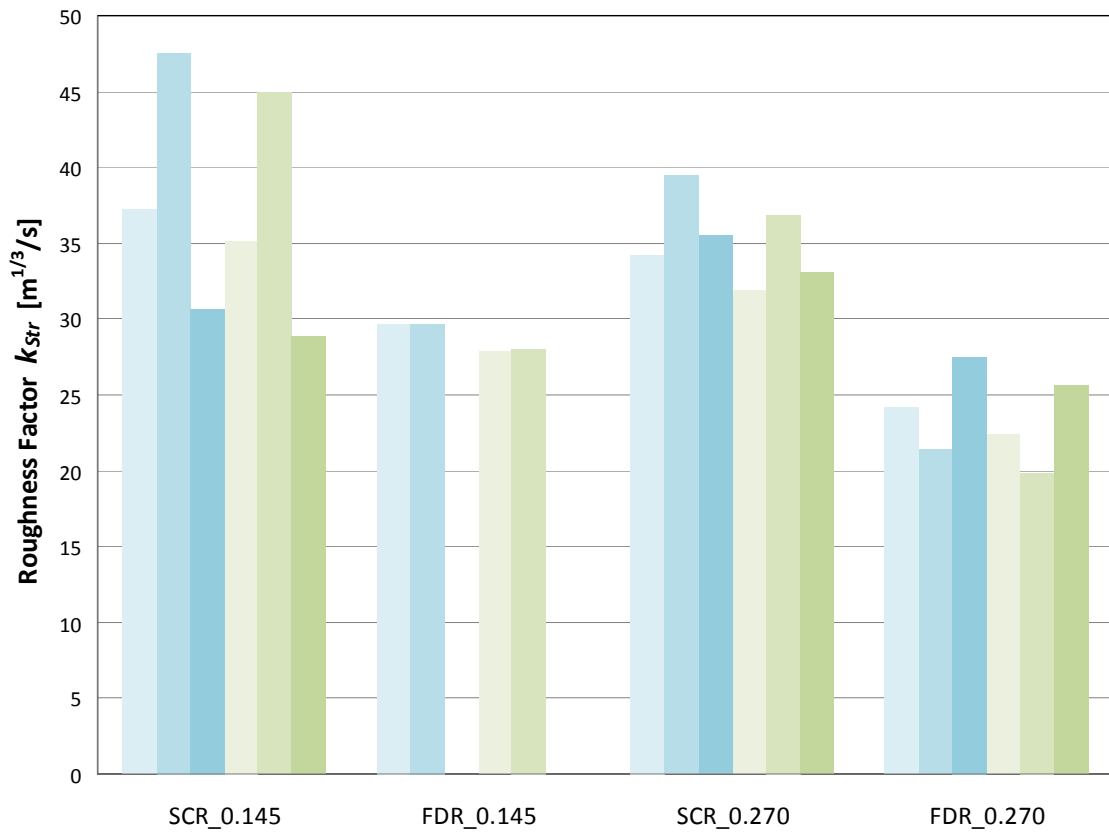
Graph 20. Calculated *Manning-Strickler-Factors* for SCR and FDR runs:
Blue and green charts represent rectangular (blue) and triangular (green)
channel cross section assumptions

Mean Results (Manning-Strickler-Factors)
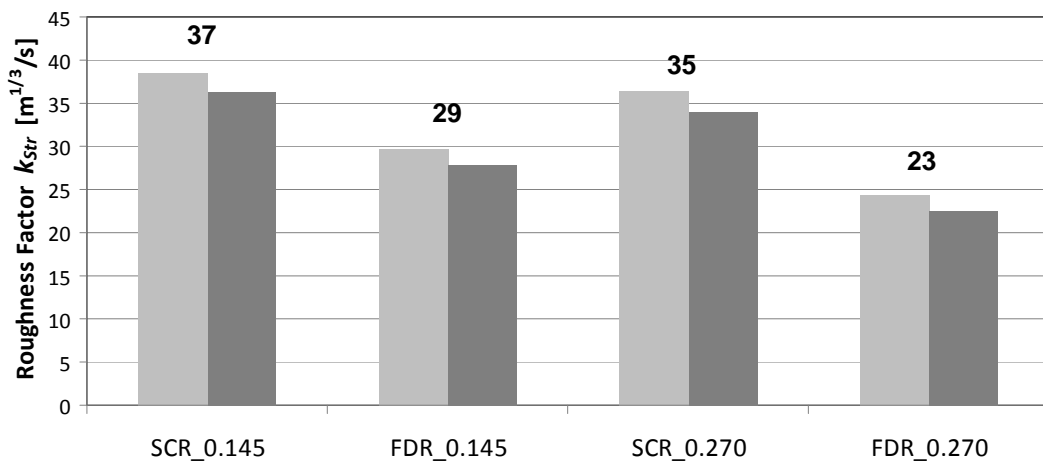
Graph 21. Calculated, averaged *Manning-Strickler-Factors* for SCR and FDR runs: a significant
increase in the *Manning-Strickler* value between SCR run and FDR run can be observed.
Bright grey charts represent rectangular cross section assumptions, dark grey charts
represent triangular cross section assumptions.

In the Graphs 20 and 21 a significant trend of the behaviour of *Manning-Strickler-Factors* is detectable. The calculated factors for the SCR experiment considering both discharges (0.145 l/s and 0.270 l/s) is about 35 to 37 in average. The factors for the FDR runs differ slightly more and are between 23 and 29 in average. The highest value for extracted *Manning-Strickler-Factor* was observed during the SCR run with 0.145 l/s of discharge. This is representing "smoothest" boundary roughness impact. The lowest roughness factor was observed during the FDR run with 0.270 l/s. Generally, the values of the SCR experiment are about 30% higher than the extracted factors of the FDR runs. Thus, a significant dependency of channel morphology to holistic roughness description may be concluded (chapter: Conclusions).

For estimating channel flow conditions for catchment size simulations referring to *Manning-Strickler* values shown in the graph 20 and 21, the following table (Tab. 5) illustrates a variety of common *Manning-Strickler* values:

Gerinnetypen	k_{St} [$m^{1/3}/s$]
Erdkanäle	
Erdkanäle in festem Material, glatt	60
Erdkanäle in festem Sand mit etwas Ton oder Schotter	50
Erdkanäle mit Sohle aus Sand und Kies mit gepflasterten Böschungen	45-50
Erdkanäle aus Feinkies, etwa 10/20/30 mm	45
Erdkanäle aus mittlerem Kies, etwa 20/40/60 mm	40
Erdkanäle aus Grobkies, etwa 50/100/150 mm	35
Erdkanäle aus scholligem Lehm	30
Erdkanäle, mit groben Steinen angelegt	25-30
Erdkanäle aus Sand, Lehm oder Kies, stark bewachsen	20-25
Felskanäle	
Mittelgrober Felsausbruch	25-30
Felsausbruch bei sorgfältiger Sprengung	20-25
Sehr grober Felsausbruch, große Unregelmäßigkeiten	15-20
Gemauerte Kanäle	
Kanäle aus Ziegelmauerwerk, Ziegel, auch Klinker, gut gefugt	80
Bruchsteinmauerwerk	70-80
Kanäle aus Mauerwerk (normal)	60
Normales (gutes) Bruchsteinmauerwerk, behauene Steine	60
Grobes Bruchsteinmauerwerk, Steine nur grob behauen	50
Bruchsteinwände, gepflasterte Böschungen mit Sohle aus Sand und Kies	45-50
Betonkanäle	
Zementglattstrich	100
Beton bei Verwendung von Stahlschalung	90-100
Glattverputz	90-95
Beton geglättet	90
Gute Verschalung, glatter unversehrter Zementputz, glatter Beton	80-90
Beton bei Verwendung von Holzschalung, ohne Verputz	65-70
Stampfbeton mit glatter Oberfläche	60-65
Alter Beton, unebene Flächen	60
Betonschalen mit 150-200 kg Zement je m^3, je nach Alter u. Ausführung	50-60
Grobe Betonauskleidung	55
Ungleichmäßige Betonflächen	50
Holzgerinne	
Neue glatte Gerinne	95
Gehobelte, gut gefügte Bretter	90
Ungehobelte Bretter	80
Ältere Holzgerinne	65-70
Blechgerinne	
Glatte Rohre mit versenkten Nietköpfen	90-95
Neue gußeiserne Rohre	90
Genietete Rohre, Niete nicht versenkt, im Umfang mehrmals überlappt	65-70
Natürliche Wasserläufe	
Natürliche Flußbetten mit fester Sohle, ohne Unregelmäßigkeiten	40
Natürliche Flußbetten mit mäßigem Geschiebe	33-35
Natürliche Flußbetten, verkrautet	30-35
Natürliche Flußbetten mit Geröll und Unregelmäßigkeiten	30
Natürliche Flußbetten, stark geschiebeführend	28
Wildbäche mit grobem Geröll (kopfgroße Steine) bei ruhendem Geschiebe	25-28
Wildbäche mit grobem Geröll, bei in Bewegung befindlichem Geschiebe	19-22

Tab. 5. *Strickle*r Factors (Nautscher, 1987):
Manning-Strickler-Factor is used in German engineering dominantly, so the table is German language. The principle behind equation [4] and the methodology is used world wide with different adoptions to the factors. The red marked area shows the values for natural river beds (k_{Str} is between 19 and 40)

6.) Conclusions

6.1.) General

General conclusions out of the Experimental Rill Erosion Development Study are:

- There is a significant dependency of channel flow conditions and channel morphology due to roughness impacts
- There is a need for itemized determination of skin and channel shape roughness

But: Such observations and claims are already investigated. Several experiments and observations affirm the results of the actual study, executed at the NSERL, West Lafayette, USA. However, as mentioned in the introduction, lack of predictability in small scale channel development and/or lack of data from the catchment inhibit proper model adoptions. The aim of the actual study was to extract the significance of insufficiency using holistic channel roughness assumption. Advanced analyses based on current flume experiment data will follow and additional future flume tests may focus on tasks like: How to predict neglected shape roughness impact due to rill morphology? Predicting morphological influence which caused more or less 30 % of holistic roughness impact during the present study, uncertainty in estimating roughness factors might be reduced.

6.2.) Model Settings, Measurements and Analysis Methods

<u>Model Set-Up</u>
Analysis of the flume study output enables a better understanding of physical process as well as possible insufficiency in model setup as the predicted model behaviour might develop unexpected.
Generally, there are always limitations in applicability of natural conditions due to physical modelling. Model boundary conditions, artificial preparation of natural conditions, which might occur in time dependency over years or at least adjustments in scale will influence model processes, which might inhibit transformation of observations into nature. According to the actual study the time limited schedule (3 month of research exchange program) caused limitations in model adjustments to natural conditions.
However, visual analysis of channel development in the flume lead to the conclusion that the model set up might provide adequate natural process characteristics. Due to relative evaluation of the results of FDR and SCR runs, possible process insufficiency decreases.

Flume Construction
The 2 meter long flume construction limits the channel development significantly. The fixed model outlet constraints the outflow in central flume area, whereas the surface water inflow at the upper flume border is dispersed over whole surface width (FDR) by means of the fleece textile of the inflow well. Nevertheless due to boundary influences the water intends to create maximum discharge in central flume regions at the inlet too. The influences of centric model outflow and more or less centric model inflow conditions impact channel meandering situation especially in case of limited model length. To create single channel development and avoid random erosion rill occurrences, the model width had to be defined too. Naturally, the shallow surface flow creates several erosion rills, depending on the hill slope topography, soil conditions, vegetation e.g. Naturally, rills develop at points of surface water concentration. The demand of the model run was to avoid interference of channel development by means of a random rough, but plain and uniform surface soil preparation without large scale preferential flow, whereas small scale obstacles like soil aggregates for sure create sheet flow dispersion. This is quite essential for creating representative rill morphology. The channel width impacts rill morphology, as side boundaries produce roughness, decrease flow velocity and inhibit widening of meander bows of the erosion

channels. The chose setup width of 35 cm represents more or less the average erodible hill slope width, provided by corn fields. Corn crop cover allows significant soil losses considering agricultural soil erosion problems. The corn row distances are usually about 0.7 m, but stabilized soil by corn crop root limit the erodible soil width per row to approximately 0.3 to 0.5 meter during the intense erodible periods of heavy summer storms but developed crop cover. In this manner, the chosen set-up width might be chosen adequately considering specific soil erosion problems in agricultural lands. Additionally, the chose flume inclination (10%) is of significant impact. Nevertheless, chosen preparations and boundary conditions provide particular studies or trends in development only.

Soil
The used loamy soil is defined by 32 % sand, 49 % silt and 19 % clay texture. As this soil origin from agricultural and urban top soil, the used soil is representative for local studies. Soil types and texture vary in large scale and worldwide, whereas this study provides soil relative analyses only. Furthermore, the soil preparation, bulk density, soil aggregates, soil pore systems, e.g. influence the soil erodibility and water infiltration characteristics significantly. Limits in soil depth (model: about 15 to 20 cm) cause increased importance of chosen infiltration boundary conditions. It was assumed to create free drainage infiltration condition by means of a perforated flume bottom and approximately 5 cm thick gravel layer below the 15 to 20 cm thick soil layer on top. In nature, different infiltration scenarios might occur due to soil compaction or low to high infiltration capacity layers. Focusing on the back-calculated infiltration rates observed during the model runs, the chosen set-up provides infiltration rates in a realistic range. The preparation of the soil aggregation must be taken into account – for the present study, a grinding of the soil aggregates to 2 cm maximum grain diameter was executed.

Discharge and Simulated Rainfall
The erosive force of the study is based on water mass and gravitation. As mentioned in chapter "general Issues in Soil Erosion", soil erosion by water consist of several processes. Erosive forces due to water occur by means of the raindrop impact and/or because of water flow forces. The decision for the present study was to concentrate on water flow forces only to avoid ambivalence in result interpretation. Future studies might include additional processes in case that single impacts of processes are detectable.
The model runs were conducted under steady state discharge conditions. The chemical water condition is of impact too because of the intention to disperse aggregates. Natural rainfall is comparable to distilled water, which is of importance during rainfall simulations. For the present channel erosion study the decision was to use standard tab water, as channel erosion processes produce high erosion rates with neglect-able influence of water chemistry. The soil preparation was done by means of simulated rainfall before each model run. This procedure causes soil water saturation, sealing of coarse soil pores to reduce infiltration capacity, compaction of the soil layer and smooth and random soil surface characteristics. For sure, the simulated rainfall intensity, absolute amount of water, rainfall duration and duration in resting time after the rainfall simulation has to be similar for every run and impacts the soil conditions. For example: Highly intense rainfall would cause surface runoff and preferential flow channels for further model runs. In this way, the soil preparation is sensitive procedure.
The model run was started by discharging the flume with 0.145 l/s respectively 0.270 l/s of surface runoff from upper flume water well source, connected to a tab water tube. For analysing the experiment focused on water flow conditions, there is a need of variation in discharge. As the model is limited in geometry and the soil characteristics provide rill erosion in dependence of soil resistance to water forces, the variation in discharge is limited too. For example: Low discharge will not be able to erode soil particles beyond a certain soil grain diameter, whereas no channel development would be enabled. Very high discharges would flush whole flume immediately without morphological influence – the experiment would be limited by boundary conditions flume construction. To hold in mind, the conflict of high

variation concerning influencing parameters for significance analysis and limitations in practicability has to be solved sensitively.

SCR and FDR set up
The study is based on allowance of and prevention against channel meandering – executed by SCR and FDR rill study settings. These meanders, step and pool sequences, changes in flow conditions e.g. impact the energy dissipation situation the roughness hypothesis is based on. Regardless the applicability of flow equations, the FDR experiment is constrained by model boundary conditions. The SCR experiment is even more critical set-up. The initial rill as central line of discharge concentration impacts the erosion regime. Artificial high flow velocities e.g. might impact further erosion development. Less material to erode in vertical source for the channel causes less accumulation of big scale gravel fraction which would create a resisting channel bottom layer and stable river bed in this way. Another argument is for sure sudden channel bank breaks which produce deviations from straight channel assumptions.

Generally, model runs are dominantly influenced by defined model assumptions. However insufficiency in applicability may result – the consistency in model run execution is essential.

Analysis Methods
Flume Measurements
During the model runs discharge, flow velocity and channel geometry data were extracted. For estimating all these parameters, different methods are available. With the aim of low influence during model runs few measuring methods remain. Especially the photogrammetric analyses based on stereo photos from above allow detailed and continuous (photo-interval of 1 minute was chosen) analyses. The disability to analyse wetted channel geometrics results in additional manual channel depth measurement requirements. Nevertheless, producing 3-D terrain models out of stereo-photos, channel width and length geometrics as well as sediment volumetric surface balances are enabled. The main advantage of this method is in the high accurate channel morphology observation and the detection of real flow path length, allowing channel tortuosity studies.
Discharge measurements were executed using bucket method. The estimation of discharge is done by measuring the outflow water volume in certain time interval. The results are expected to be of sufficient accuracy.
Flow velocity measurements by tracer method include the big advantage of marginal influences on flow compared to vane meter for example. The accuracy of the method has been discussed in this paper. Relating to representativeness due to averaging the variable flow conditions over channel length and channel cross section using colour tracer seems to be most practical method.
Sediment concentration was measured by means of 1 liter sample bottles every minute of the model run. This allows detailed resolution in sediment concentration behaviour. As the 1 liter bottles take about 4 to 8 seconds to fill the probe every minute, with this method about 10% of the whole outflow was observed.
Concerning flume measurements in general the combination of measurement accuracy and representativeness has to be achieved.

Analysis Methods
To compare common hypothesis concerning roughness consideration in channel flow equations, adequate accurate measuring of related parameters is essential. On the other hand, the applicability of the hypotheses is basic requirement. Assuming the analysed *Manning-Strickler-Equation* [4] describes channel flow conditions adequately, additional simplifications have to be defined.
Especially channel flow path and channel cross section assumptions are hardly definable. Flow path length is important input for average channel slope and tortuosity estimation. As the flow path is hard to define in theory - for example: Path of highest stream directed velocity (but which scale?) the stream line detection in case of photo images is even more

complicated. However, comparing different photo digitisations of possible flow paths results varied marginal in present channel scale. This conclusion might be adequate for channel length estimations concerning real channel slope, but in case of tortuosity calculations the inaccuracy in flow path definition may be of significant impact. The results of the analyses and the interpretation on the results are discussed following.

6.3.) Results

Channel Development Observations
Observed channel morphology development showed comparable characteristics to natural rill erosion occurrences. Regardless channel morphology dependencies from soil, discharge and preparation, wide section of the developed channel seemed to be low influenced by flume boundary.
The FDR channel development initiated at the rim of the pothole shaped outlet situation. Primarily, the water eroded the edge at the outlet cone. Furthermore small scale preferential flow of shallow sheet flow created small rill path connected to the topographical step at the cone outlet. After small scaled rill development at the plain soil surface even more water concentrated into these locations. Because of local water depth increase the flow velocity increased too, whereas more water was able to be routed. As a consequence, deepening into preferential flow occurred and channel formation started as back-cut erosion from the knick point in soil surface at the outlet. The FDR step of the back-cutting knick-point remained more or less constant in height during this process. The reason for remaining topographical step during back-cut erosion is in the pothole at the point of channel formation beyond the back-cut step. On one hand, the surface water flowing upon the rim of the knick-point intends to smoothen out the sharp edge between soil surface and steep front of the upper channel border. On the other hand, the water turbulence at the pothole underneath the knick-point causes bank erosion at the foot of the step. Because of this, sudden bank breaks occur resulting in back-cut erosion. This phenomenon was observed in field gully erosion processes as well. The comparability to natural channel respectively gully development points out the reliability of the rill erosion study results.

Channel Flow Conditions
The assumed representativeness of discharge, channel flow velocity and sediment concentration measurements was already discussed. The channel flow conditions were measured in averaged way as mean values for certain channel section (about 1.3 m length). Observed meanders, changes from under critical to supercritical conditions and local energy dissipation due to hydraulic jumps clearly show the insufficiency of such approaches. In this way, the hypothesis of uniform flow conditions has to be questioned. However, assumptions of section wise uniformity are common in erosion modelling; the sensitivity of lack of applicability will be argued during this model study.
From the point of view of flow transition, the *Froude Numbers* might be critical value. In chapter "Introduction in Results and Analyses (current stage)" the importance of this value was discussed. The value of 1.0 describes the critical point between under critical (below 1.0) and supercritical (above 1.0). Whereas changes from under critical to supercritical are hardly detectable by eye and have hardly impact on energy dissipation, hydraulic jumps caused by changes from super to under critical flow conditions result in local turbulence and energy dissipation. Chapter "Experimental Data Summary" shows back calculated *Froude Numbers*. Particularly average values about 1.0 in combination with observed high tortuosity (meanders, step and pool) refer to flow condition changes and local energy dissipation. Focusing in FDR experimental runs (SCR is straight channel without remarkable changes in channel uniformity) back calculated values are (also see in Tab. 4) FDR 0.145 l/s: 1.1 / 1.1 rectangular cross section and 0.8 / 0.8 for triangular CS ; FDR 0.270 l/s: 0.8 / 0.8 / 1.0 for rec. CS and 0.6 / 0.5 / 0.7 tri. CS. This describes the affinity of channel flow conditions to operate hydraulic jumps. In contrast, the SCR flow is assumed to behave uniform – less energy dissipation is the result.

Furthermore, the *Reynolds Number* is indicator value for flow conditions: laminar or turbulent. Generally, open channel flow is turbulent flow. Very shallow channel flow intends to low flow velocities because of huge boundary roughness impact. Under very shallow flow depth conditions, changeover to laminar flow (as defined by *Reynolds* values below ≈ 2300) might occur. Referring to Tab. 4 *Reynolds Numbers* below 2300 occur in the 0.145 l/s discharge experiments under rectangular channel cross section assumptions only. All the other back calculated *Reynolds Numbers* are estimated in turbulent flow range. The flow condition – laminar or turbulent – is critical point, as the related flow hypotheses change remarkable. In laminar flow, the flow resistance force is based on inner fluid friction (viscosity) only because of assumed parallel flow vectors and is in direct proportion to average flow velocity. In turbulent flow, lateral flow accelerations occur (turbulence) and the flow resistance forces are of inner and boundary friction, whereas foremost boundary forces are of major impact. The friction forces behave proportional to the squared average channel flow velocity. Several flow relations like the *Manning-Strickler-Equation* define the flow by boundary roughness only. However, based on common *Reynolds Number* definition of critical value of 2300, shallow channel flow occurring in rill erosion processes seem to be borderline situations of open channel hydraulic assumptions due to the choice of flow equations.

Channel Roughness
Equation [4] illustrates the *Manning-Strickler* assumption to account for holistic roughness impact relating to uniform open channel flow. Because of application of this equation [4] by means of common catchment size erosion models (for example: WEPP software) the actual flume study was executed to back calculate roughness impact and to point out the applicability due to channel morphological influence. Tab. 3 and Graph 20 illustrate the variability of *Manning-Strickler-Factors*. The clear trend of decreasing values by up to 30% in case of natural meandering rills (FDR) verifies significant insufficiency of this method. The following images will illustrate the significance related to natural channel roughness definition in river scale:
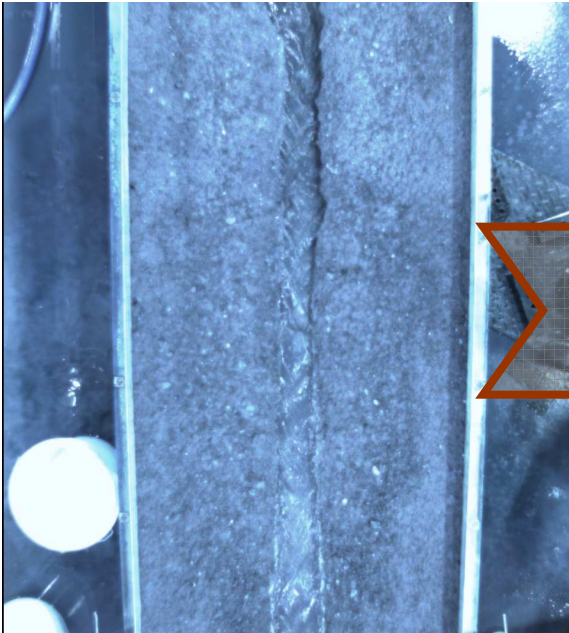
MODEL   **NATURE**

Fig. 45. Model experiment run SCR 0,145 l/s: extracted Manning-Strickler value ≈ 35

Fig. 46. Natural (shored) river: estimated shored) river: estimated Manning-Strickler value ≈ 30-35

MODEL	NATURE

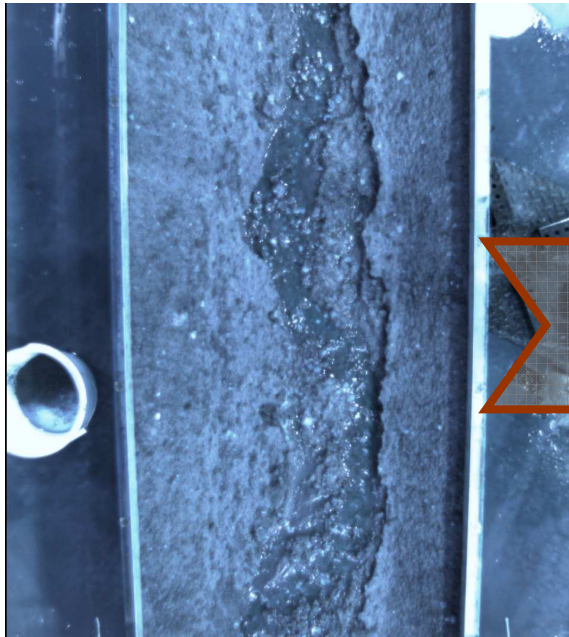

Fig. 47. Model experiment run FDR 0,145 l/s: extracted Manning-Strickler value ≈ 25

Fig. 48. Natural alpine river: estimated shored) river: estimated Manning-Strickler value ≈ 20-25

As illustrated in Figures 45 to 48, changes from *Manning-Strickler-Factors* from about 25 to 35 describe significant differences for natural scenarios. Serious river engineering structures – if based on holistic roughness assumptions at all – are calculated by means of a range of realistic parameters and worse case scenarios. Nevertheless, realistic estimations of acting forces are essential for proper conservation techniques. The valuation respectively the prediction of channel morphologic impact on roughness seems to be required based on actual the rill erosion study observations.

Channel Erosion and Sediment Transport
The development of the erosion channels was comparable to natural rill or emepherial gully erosion characteristics. In this way, the sediment erosion processes might behave similar – the channel development is in direct dependency to soil erosion processes. Although the sediment transport is not main focus of the present study, the observation of sediment concentration during the model runs is critical process.
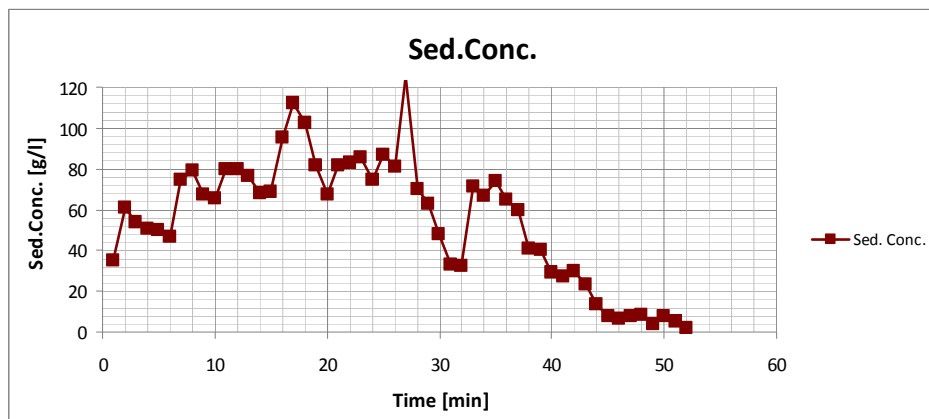
Graph 22. The grapg shows the sediment concentration Of the FDR 0,145 l/s experiment

Describing Graph 22, the sediment concentration at the outlet fluctuates. The sediment concentration measured in 1 minute interval by 1 liter sample bottles shows increasing trend (although fluctuating) until the upper boundary of the flume is reached by back-cut erosion. Reaching the upper boundary (about minute 27 in graph 17) a last significant peak in sediment concentration is detectable because of sudden soil breaks at the steep metal sheet boundary. After this, the channel deepens and widens, whereas the sediment concentration decreases in general. The point, when the deepening of the channel declines sediment concentrations shows more or less stable and low values (about minute 45 to 50 in graph 17). This stage was defined as stable state of channel morphology, where acting forces of the channel water flow is in equilibrium with soil resistance forces due to decrease in slope steepness and lower flow velocities. This situation was the compared flow condition (SCR and FDR), because of the differences in boundary impacts and development during different SCR and FDR runs. The fluctuation in sediment concentration illustrated in Graph 22 exemplarily is based on sudden bank breaks in back-cut erosion as well because of breaks in meander curves due to acting forces of the water flow.

6.4.) Future Prospects

Model study data of the Experimental Rill Erosion Development Study at the NSER, West Lafayette, USA provide a wide range of possible future analysis.
Preliminary studies focussing on flow conditions of different model runs point out basic insufficiencies in simplified channel flow assumptions used in rill erosion scale.

Advanced analyses may concentrate on testing different relations between measured parameters - for example: Channel tortousity, flow velocity and the morphological rill development. Primary approaches will be based on parameter regressions.

Sediment concentration observations contain detailed data information. Fluctuations in sediment concentration might be explainable using *Fourier Row* methods. These statistical approaches describe fluctuations in measurements by means of oscillating functions. Herewith, lack of predictability might be reduced and a deeper insight in the meander erosion problematic might be provided. The use of oscillating functions may be justified based on the boundary erosion processes and sudden bank breaks of certain characteristic.

Furthermore, the stereo pictures provide huge data amount to analyze. GIS tool flow path studies may follow or balances between DEM sediment budgeting compared to bottle sediment concentration. Channel geometric characteristics may be analyzed in an advanced way.

In Summary….
Based on the rill erosion study at the NSERL testing of hydrodynamic hypotheses is enabled – furthermore, novel relations and characteristics may be described by means of actual model observations.
For the future, advanced flume model studies are discussed to be performed at the Hydraulic Laboratory of the BOKU University.

References

1. Kinnell, P.I.A., 2005. Sediment transport by medium to large raindrops impacting flows at subterminal velocity. *Soil Sci. Soc. Am. J.* 69: 902-905.

2. Bennet, S.J., C.V. Alonso, S.N. Prasad, and M.J.M. Römkens, 2000. Experiments on headcut growth and migration in concentrated flows typical of upland areas. Water Resour. Res. 36: 1911-1922

3. Slattery, M.C., and R.B. Bryan, 1992. Hydraulic conditions for rill incision under simulated rainfall: A laboratory experiment. Earth Surf. Processes Landforms 17: 127-146

4. Wells, R.R., C.V. Alonso, and S.J. Bennet, 2009. Morphodynamics of Headcut Development and Soil Erosion in Upland Concentrated Flows. *Soil Sci. Soc. Am. J.* 73: 521-530.

5. Brunton, D.A., and R.B. Bryan, 2000. Rill Network development and sediment budgets. Earth Surf.Processes Landforms 25: 783-800

6. Valentin, C.J., J. Poesen, and Y. Li, 2005. Gully erosion: Impacts, factors and control. Catena 63: 132-153

7. Loiskandl, W., 2011. University Lecture Script: "Hydrodynamik", University of Natural Resources and Life Sciences, Institute of Hydraulics and Rural Water Management, 2011

8. Flanagan, D.C., J.C. Ascough, A.D. Nicks and J.M. Laflen, 1995. USDA-Water Erosion Prediction Project, Hillslope Profile and Watershed Model Documentation. NSERL Report Nr. 10, July 1995

9. Website: ASA-CSSA-SSSA, 2011, https://www.soils.org/ , visited on December 10th 2011

10. Website: Wikipedia, 2011, http://en.wikipedia.org/wiki/Soil , visited on December 10th 2011
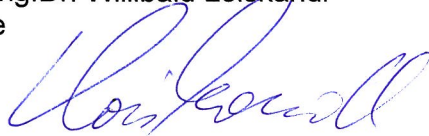
Approbation

The present report confirms the goal-oriented research work based on the abroad research stay of the PhD Student DI Stefan Strohmeier at the Purdue University, West Lafayette from 1st of Aug 2011 to 31st of Oct 2011.

Certified herewith, the appointed requirements of the exchange program funded by the Marshallplan-Jubiläumsstiftung are achieved completely.

Institute of Hydraulics and Rural Water Management
Dept. Water, Atmosphere, Environment
BOKU Vienna, Muthgasse 18, 1190 Vienna

Univ.Prof.Dipl.-Ing.Dr. Willibald Loiskandl   Jan. 2012
Head of Institute